Maternal obesity may disrupt offspring metabolism by inducing oocyte genome hyper-methylation via increased DNMTs

Shuo Chao[1#], Jun Lu[1#], Li-Jun Li[1], Hong-Yan Guo[1], Kui-Peng Xu[2], Ning Wang[1], Shu-Xian Zhao[1], Xiao-Wen Jin[1], Shao-Ge Wang[1], Shen Yin[1], Wei Shen[1], Ming-Hui Zhao[1], Gui-An Huang[1], Qing-Yuan Sun[3*], Zhao-Jia Ge[1*]

1. College of Life Sciences, Institute of Reproductive Sciences, Key Laboratory of Animal Reproduction and Germplasm Enhancement in Universities of Shandong, Qingdao Agricultural University, Qingdao 266109, P. R. China;

2. College of Horticulture, Qingdao Agricultural University, Qingdao 266109, P. R. China;

3. Guangzhou Key Laboratory of Metabolic Diseases and Reproductive Health, Guangdong-Hong Kong Metabolism & Reproduction Joint Laboratory, Reproductive Medicine Center, Guangdong Second Provincial General Hospital, Guangzhou 510317, China.

# These authors contributed equally to this work.

* Corresponding author: Zhao-Jia Ge

College of Life Sciences, Qingdao Agricultural University,

Qingdao 266109, P. R. China; +86 15588647272

Email: gejdssd313@163.com; zjge@qau.edu.cn

Qing-Yuan Sun

Reproductive Medicine Center, Guangdong Second Provincial General Hospital, Guangzhou 510317, China. sunqy@gd2h.org.cn.

Abstract

Maternal obesity has deleterious effects on the process of establishing oocyte DNA methylation; yet the underlying mechanisms remain unclear. In the present study, we found that maternal obesity induced by high-fat diet (HFD) disrupted the genomic methylation of oocytes, and that at least a part of the altered DNA methylation was transmitted to the F2 oocytes and the livers via females. We further examined the metabolome of serum and found that the altered metabolites such as melatonin may play a key role in the disrupted genomic methylation in the oocytes of obese mice. We further found that exogenous melatonin treatment significantly reduced the hyper-methylation of HFD oocytes, and the increased expression of DNMT3a and DNMT1 in HFD oocytes was also decreased. To address how melatonin regulates the expression of DNMTs, the function of melatonin was inhibited or activated upon oocytes. Results revealed that melatonin may regulate the expression of DNMTs via the cAMP/PKA/CREB pathway. These results suggest that maternal obesity induces genomic methylation alterations in oocytes, which can be partly transmitted to F2 in females, and that melatonin is involved in regulating the hyper-methylation of HFD oocytes by increasing the expression of

DNMTs via the cAMP/PKA/CREB pathway.

Keywords: Obesity, oocyte, methylation, melatonin, cAMP/PKA/CREB pathway

Introduction

Obesity has become a global health problem, affecting approximately 13% of the world's adult population, and over 340 million children and adolescents (WHO). This epidemic has profound implications not only for reproductive health but also for the well-being of subsequent generations. Previous studies have demonstrated that maternal obesity reduces the function of the hypothalamic-pituitary-ovarian (HPO) axis (X. Chen, Xiao, Cai, Huang, & Chen, 2022), deteriorates oocyte cytoplasmic quality and nuclear maturation, and disrupts genome methylation (Broughton & Moley, 2017). Reduced expression of *Stella* in oocytes induced by obesity results in global hypo-methylation in zygotes, which has an important contribution to the defective embryo development (Han et al., 2018). Furthermore, progeny of obese females have a higher risk of non-communicable diseases, such as obesity, diabetes, and cardiovascular diseases (Godfrey et al., 2017). Our previous study indicated that obesity altered the methylation status of *Leptin*, which might play a role in the metabolic disorders of female offspring. However, these methylation changes are not detected in the first-generation (F1) oocytes (Ge et al., 2014). The influence of maternal obesity on the genomic methylation of oocytes is still obscure. Thus, more studies

are necessary to explore the role of DNA methylation in mediating the transgenerational transmission of metabolic syndrome induced by female obesity.

Obesity also perturbs glucose and lipid metabolism, which has negative effects on oocyte maturation and embryo development. Elevated levels of circulating free fatty acids in obese females contribute to oocyte lipotoxicity, while concomitantly diminishing mitochondrial function within oocytes (Broughton & Moley, 2017). The decreased melatonin levels are also reported in animals and humans by previous studies (Overberg et al., 2022; Virto et al., 2018). Melatonin has contributions to metabolism and DNA methylation in somatic cells (Davoodvandi, Nikfar, Reiter, & Asemi, 2022). These findings indicate that the disturbed metabolism induced by obesity is closely linked to the compromised oocyte quality and aberrant methylation patterns. This study aims to elucidate the effects of obesity-induced metabolic changes on oocyte genomic methylation and its inhereditary implications in a murine model.

Results

Obesity alters the genomic methylation in oocytes

The obese mouse model was induced via a high-fat diet (HFD) (Ge et al., 2014; Han et al., 2018), and mice fed with standard diet were used as a control (CD). The HFD group exhibited a significantly higher average body weight compared to CD group (n>86, Fig. S1A and B). Re-

methylation in oocytes occurs in follicular development and is nearly complete at the germinal vesicle (GV) stage. The 5mC (5-methylcytosine) and 5hmC (5-hydroxymethylcytosine) levels in the GV oocytes of HFD mice were significantly higher than that in the CD group (n>30, Fig. 1A-C). To further explore the effects of maternal obesity on the oocyte methylation, we examined the genomic methylation of metaphase II (MII) oocytes using whole-genome bisulfite sequencing for small samples (WGBS, Novogene, Beijing, China). The information of reads count, mapping rate, conversion rate and sequencing depth was presented in Table S1. We found that global methylation in MII oocytes of HFD group was higher than that in the CD group (Fig. 1D). Methylated cytosine (C) can be classed into three types according to the context in the genome including CG, CHG and CHH (H=A, T or C). The methylated CG have more contributions to regulate gene expression. We found that the CG methylation level in MII oocytes of HFD was significantly higher than that in the CD group (Fig. 1E). Differentially methylated CG distributed across all chromosomes (Fig. S1C). To further analyze the distribution of methylation, each functional region of genes was equally divided into 20 bins, and then the average methylation levels in the functional regions were calculated, respectively. CGIs (CG islands) and CGI shores were predicted using cpgIslandExt and repeat sequences were predicted using RepeatMasker. Results showed that the hyper-methylation was distributed

109 in the promoter, exon, upstream 2k, and downstream 2k regions (Fig. 1F
110 and Fig. S1D) of genes in HFD oocytes. These findings suggest that
111 maternal obesity results in hyper-genome methylation in oocytes.

112 **Distribution of differentially methylated regions (DMRs)**

113 We further analyzed the differentially methylated regions (DMRs) in
114 oocytes, and identified 4340 DMRs between HFD and CD oocytes. These
115 DMRs were defined by the following criteria: the number of CGs ≥ 4 and
116 the absolute methylation difference ≥ 0.2. Among these, 2,013 were hyper-
117 DMRs (46.38%), and 2327 were hypo-DMRs (53.62%) (Fig. 1G). These
118 DMRs were distributed across all chromosomes (Fig. 1H). We then
119 annotated DMRs into different genomic regions including promoter, exon,
120 intron, CGI, CGI shore, repeat, TSS (transcription start site), TES
121 (transcription end site), UTR3 (3' end untranslated region), and UTR5 (5'
122 end untranslated region) regions (Fig. S2A), and the average methylation
123 levels of DMRs in these regions were similar between HFD and CD
124 oocytes (Fig. S2B). However, the hypo-DMRs were enriched in the UTR3,
125 repeat, and intron regions compared with hyper-DMRs (Fig. S3).

126 Methylation level at promoters strongly contributes to the regulation of
127 gene expression. We then analyzed the enrichment of genes with DMRs at
128 promoters in KEGG (Kyoto Encyclopedia of Genes and Genomes)
129 pathways using KOBAS online. Results indicated that the genes with
130 DMRs at promoters were significantly enriched in metabolic pathways

including amino acid metabolism pathways, carbohydrate metabolism pathways, lipid metabolism pathways, and metabolism of cofactors and vitamins pathways (Fig. 1I, Table S2). A total of 35 genes with DMRs at promoters were included in metabolism pathways, and 19 of these genes were with hyper-DMRs and 16 of these genes were with hypo-DMRs (Table S3). These results suggest that the altered methylation in oocytes induced by maternal obesity may play a role in the metabolic disorders in offspring.

The disturbed methylation may be associated with the transgenerational inheritance of the metabolic disorders through females

Our recent study demonstrated that disturbed methylation in oocytes caused by uterine undernourishment can be partly transmitted to F2 oocytes via females, which may play a key role in the transgenerational inheritance of metabolic disorders (S. B. Tang et al., 2023). Here, we investigated the inheritance of altered methylation in HFD oocytes. F1 and F2 generations were produced as shown in the schedule in Fig. 1J: HF1 and CF1, female HFD and CD, respectively, were mated with control males; HF2 and CF2, female HF1 and CF1, respectively, were mated with control males. We examined the glucose and insulin tolerance (GTT and ITT), and found that the GTTs and ITTs of F0, F1, and F2 females were impaired (Fig. 2A-C). The inheritance of disrupted metabolism in females

153 might be associated with the altered DNA methylation of oocytes. To
154 address this question, we first examined the DNA methylation status of
155 DMRs located at the promoters of *Bhlha15* (also known as *Mist1*, basic
156 helix-loop-helix, a transcription factor), *Mgat1* (mannoside
157 acetylglucosaminyltransferase 1), T*aok3* (serine/threonine-protein kinase
158 3), *Tkt* (transketolase), *Pik3cd* (phosphatidylinositol-4, 5-bisphosphate 3-
159 kinase catalytic subunit delta), and *Pld1* (phospholipase D1) in the HFD
160 and CD oocytes. We found that the methylation levels of hyper-DMRs
161 including *Bhlha15*-DMR, *Mgat1*-DMR, and *Taok3*-DMR in HFD oocytes
162 were significantly higher than in the CD group (Fig. 2D). The methylation
163 level of hypo-DMRs, *Pik3cd-DMR* in HFD oocytes was significantly lower
164 than that in the CD group (Fig. 2D). These results coincide with the
165 genomic sequencing results. Whereas, the methylation level of *Tkt-DMR*
166 (hypo-DMR) in HFD oocytes was higher than that in the CD group, and
167 the methylation level of *Pld1-DMR* (hypo-DMR) was similar between the
168 two groups, which contradicts the genomic sequencing results (Fig. S4A).
169 These findings suggest that some regions are false positives in genomic
170 sequencing. To exclude the effects of somatic cell contamination, we
171 examined the methylation level of paternally imprinted gene *H19,* which
172 was low in both HFD and CD oocytes (Fig. S4B). These findings indicate
173 that the samples are not contaminated by somatic cells.
174 We then examined the methylation of DMRs in F1 livers using bisulfite

175 sequencing (BS). Ten livers from five litters were analyzed for each group.
176 Results revealed that the methylation levels of *Bhlha15*-DMR and *Mgat1*-
177 DMR were higher and the methylation level of *Pik3cd*-DMR was lower in
178 HF1 livers than that in CF1 livers (Fig. S5A-C). The methylation level of
179 *Tkt-DMR* in HF1 livers was lower than that in CF1 (Fig. S5D), although it
180 was higher in HFD oocytes compared with CD. This contradiction may be
181 associated with the uterine environment of obesity and the reprogramming
182 during early embryo development. We further examined the expression of
183 several genes with DMRs at promoters, including hyper-methylated genes,
184 such as *Bhlha15*, *Mgat1*, *Dgka*, *Pdpk1* and *Taok3*, and hypo-methylated
185 genes, such as *Igf1*, *Map3k8*, *Pld1*, *Tkt*, *Pik3cd* and *Sphk2*. The expression
186 levels of *Bhlha15*, *Mgat1* and *Pdpk1* were significantly lower and the
187 expression levels of *Map3k8*, *Tkt*, *Pik3cd*, and *Sphk2* were significantly
188 higher in HF1 livers compared to that in CF1 (Fig. S5E and F). The
189 expression trends of *Bhlha15*, *Mgat1*, *Tkt*, and *Pik3cd* were consistent with
190 the methylation status at promoters in F1 livers. The expression of *Dgka*,
191 *Taok3*, *Igf1*, and *Pld1* was not affected in F1 livers (Fig. S4E and F). *Mgat1*
192 is associated with lipid metabolism and obesity (Jacobsson et al., 2012;
193 Johansson et al., 2010), *Tkt* regulates glucose metabolism (Bartakova et al.,
194 2016; Kang et al., 2018), and *Pik3cd* is involved in lipid metabolism and
195 diabetes (Hood, Berger, Freedman, & Law, 2019; Wojcik et al., 2014).
196 These results suggest that the altered methylation in HFD oocytes is partly

197 transmitted to F1 livers via oocytes, and that the abnormal methylation may
198 be a reason for the disturbed metabolism of HF1.
199 If the altered methylation in HFD oocytes was inherited by HF1 oocytes,
200 it would be transmitted to F2 generation. Therefore, we examined the
201 methylation of DMRs in F1 oocytes, and results revealed that *Bhlha15*-
202 DMR, *Mgat1*-DMR, and *Taok3*-DMR were significantly hyper-methylated
203 in HF1 oocytes compared with CF1 oocytes (Fig. 2E). The methylation
204 level of *Tkt*-DMR was significantly lower (Fig. S6), and the methylation
205 level of *Pik3cd*-DMR was slightly lower in the HF1 oocytes than that in
206 the CF1 oocytes (Fig. 2E). These results indicate that at least a part of the
207 altered methylation in HFD oocytes is transmitted to F1 oocytes via
208 females.
209 To confirm the transgenerational inheritance of the altered DNA
210 methylation in HFD oocytes, we examined the methylation levels of DMRs
211 in F2 livers. The methylation of *Bhlha15*-DMR and *Mgat1*-DMR was
212 higher and the methylation level of *Pik3cd*-DMR was lower in HF2 livers
213 than that in CF2 livers (Fig. S7A-C). The methylation of *Tkt*-DMR in HF2
214 livers was similar to that in CF2 group (Fig. S7D). In addition, the
215 expression levels of *Bhlha15*, *Pdpk1*, and *Mgat1* were significantly lower
216 (Fig. S7E), and the expression levels of *Pld1*, *Pik3cd*, and *Sphk2* were
217 significantly higher in HF2 livers than that in CF2 (Fig. S7F). The
218 expression of the other gene were similar in the livers between HF2 and

219 CF2 (Fig. S7E and F). These results suggest that at least a part of the altered
220 methylation in HF2 livers may be inherited from HFD oocytes, and that
221 this alteration may be associated with the disrupted metabolism in F2
222 offspring.
223 We then examined the methylation of DMRs in F2 oocytes using BS, and
224 found that the hyper-methylation of *Bhlha15*-DMR, *Mgat1*-DMR, and
225 *Taok3*-DMR, and the hypo-methylation of *Pik3cd*-DMR and *Tkt*-DMR
226 were maintained in HF2 oocytes (Fig. 2F).
227 To better understand the inheritance of the altered methylation, we
228 analyzed the methylation level of DMRs among generations compared
229 with that in HFD oocytes (Fig. 2G). For hyper-DMRs, the methylation of
230 *Bhlha15*-DMR was maintained from HFD oocytes to HF2 oocytes.
231 Compared to those in HFD oocytes, the methylation levels of *Mgat1*-DMR
232 and *Taok3*-DMR were partly transmitted to HF2 oocytes. For hypo-DMRs,
233 the methylation levels of *Tkt*-DMR and *Pik3cd*-DMR in HFD oocytes were
234 inherited by HF2 (Fig. 2G). . We did not examine the methylation level of
235 *Pld1*-DMR in F1 and F2 because it was similar in oocytes between CD and
236 HFD (Fig. 2G). These results suggest that only a part of the altered
237 methylation in HFD oocytes can be transmitted to F2 oocytes, and that
238 disrupted methylation may be a reason for the inheritance of the metabolic
239 disorders in F1 and F2.
240 **Obesity alters the metabolomics of serum**

241 Obesity alters the metabolism of glucose, fatty acids, and amino acids,
242 which are essential for oogenesis. Thus, we suppose the altered metabolism
243 may play a key role in the disturbed global methylation in HFD oocytes.
244 We examined the metabolomics of serum using non-targeted approaches
245 (BGI, Wuhan, China). We used LC-MS/MS to identify the variation in
246 metabolites, including amino acids, carbohydrates, lipid, and phenols. The
247 principal component analysis (PCA) showed that the PC1 and PC2,
248 respectively, explained 44.6% and 9.96% of the total metabolite variation,
249 respectively (Fig. 3A). The distribution of extracts between groups was
250 distinguishable (Fig. 3A). We identified 538 differential metabolites based
251 on the PLS-DA (robust orthogonal partial least squares-discriminant
252 analysis) and T-test analysis with the following criteria: VIP (variable
253 importance in projection) $\geqslant 1$, fold change $\geqslant 1.2$ or $\leqslant 0.83$, and p-
254 value<0.05, including 288 upregulated and 250 downregulated metabolites
255 (Fig. 3B). The enrichment of differential metabolites was analyzed using
256 KEGG, which revealed that differential metabolites were significantly
257 enriched in tryptophan and vitamin B6 metabolism (Fig. 3C). The top 20
258 differential metabolites were presented in Fig. 3D. These results suggest
259 that obesity disturbs the metabolomics of serum.

260 **Melatonin may play a key role in the genomic hyper-methylation of**
261 **HFD oocytes**

262 To investigate the associations between the metabolites and methylation in

263 oocytes, we identified several differential metabolites in HFD mice,
264 including pyridoxine (vitamin B6), L-methionine, melatonin, and L-
265 tyrosine, which may be associated with the hyper-methylation of oocytes.
266 The concentration of pyridoxine (vitamin B6), L-methionine, and L-
267 tyrosine was significantly increased in HFD serum compared with CD
268 group (Fig. 3D-G). In the methionine cycle, methionine
269 adenosyltransferase catalyzes methionine and ATP into S-adenosyl
270 methionine (SAM) (Shou, Pan, & Chin, 1969) which acts as a universal
271 methyl donor (Lyon, Strippoli, Fang, & Cimmino, 2020). DNA
272 methyltransferases (DNMTs) transfer the methyl group to cytosine and
273 convert SAM to S-adenosyl homocysteine (SAH) which is further
274 degraded to homocysteine (HCY) by SAH hydrolase (D. H. Chen, Wu,
275 Hung, Hsieh, & Li, 2004). During these processes, vitamin B6 serves as a
276 co-factor (Vaccaro & Naser, 2021). Excessive methionine and vitamin B6
277 intake has been reported to induce hyper-methylation (R. A. Waterland,
278 2006). These findings indicates that the hyper-methylation in HFD oocytes
279 may be associated with the increased concentrations of methionine and
280 pyridoxine. To confirm this hypothesis, we examined the concentrations of
281 SAM, SAH, and HCY in livers and oocytes, which are crucial intermediate
282 metabolites in the methionine cycle. Results showed that the
283 concentrations of SAM, SAH, and HCY in HFD livers were similar to
284 those in CD livers (Fig. 3H-J), and the concentration of SAM in HFD

285 oocytes was lower than that in the CD group (Fig. 3K). These results
286 suggest that the higher concentrations of methionine and pyridoxine in the
287 serum of HFD mice may not be the main reason for the genomic hyper-
288 methylation in oocytes.
289 As presented in Fig. 3D, it is curious that the abundance of genistein,
290 daidzein and dibutylpthalate were also altered in HFD serum compared
291 with those in CD, which might have contributed to the altered DNA
292 methylation in the oocytes. These metabolites might be from the diets or
293 materials used to collect samples. To confirm these results, we examined
294 the concentrations of genistein and dibutylpthalate using ELISA. The
295 results revealed that the concentrations of these metabolites were similar
296 between HFD and CD serum (Fig. S8), which suggest that these
297 metabolites may have no effect on the altered methylation in oocytes.
298 As presented in Fig. 3D and L, the concentration of melatonin in the HFD
299 serum was significantly lower than that in the CD group. Low
300 concentration of melatonin has also been reported in obese rats (Virto et al.,
301 2018) and humans (Overberg et al., 2022). Exogenous melatonin
302 supplementation reduces body weight and improves lipid and glucose
303 metabolism in both animals and humans (Guan, Wang, Cao, Dong, & Chen,
304 2021). Melatonin can also inhibit cancer by regulating DNA methylation
305 status (Davoodvandi et al., 2022), improve DNA methylation
306 reprogramming in the development of porcine cloned embryos (Qu et al.,

307 2020), and affect DNA re-methylation in oocytes (Lan et al., 2018;
308 Saeedabadi, Abazari-Kia, Rajabi, Parivar, & Salehi, 2018; Xiao et al.,
309 2019). This indicates that the reduced melatonin may contribute to the
310 hyper-methylation of HFD oocytes. Here, we found that if HFD mice were
311 treated with exogenous melatonin for 14 days, the genomic hyper-
312 methylation in HFD oocytes was significantly reduced (n≥96 Fig. 3M and
313 N). These results suggest that the reduced melatonin concentration may be
314 involved in regulating the hyper-methylation of HFD oocytes.

315 **Melatonin regulates genomic methylation of oocytes by increasing the**
316 **expression of DNMTs via the cAMP/PKA/CREB pathway**

317 Melatonin receptors (MT1 and 2), which are coupled with inhibitor G-
318 protein (Gi), have been identified in oocytes and granulosa cells (Jin et al.,
319 2022; Wang et al., 2021). Activated Gi inhibits the activation of adenylyl
320 cyclases (ADCYs), resulting in a decrease of cAMP (cyclic adenosine
321 monophosphate), which regulates the activation of protein kinase A (PKA)
322 and CREB (cAMP response element-binding protein) (Wongprayoon &
323 Govitrapong, 2021). Elevated cAMP level increases the expression of
324 DNMTs resulting in hyper-methylation in HL-1 cardiomyocytes (Fang et
325 al., 2015). Hedrich *et al*. reported that CREMα induced hyper-methylation
326 of CD8 cluster via increasing the expression of DNMT3a (Hedrich et al.,
327 2014). We thus supposed that melatonin may regulate genomic methylation
328 in oocytes via increasing the expression of DNMTs through the

329 cAMP/PKA/CREB pathway (Fig. 4A). To confirm this hypothesis, female
330 C57BL/6 mice fed with normal diet were treated with luzindole, an
331 inhibitor of melatonin receptor, and the global methylation of 5mC and
332 5hmC was significantly increased in oocytes (n≥49 Fig. 4B-D). Luzindole
333 did not affect the concentration of melatonin in the serum (Fig. S9A).
334 However, excessive melatonin treatment significantly increased the
335 concentration of melatonin in the serum (Fig. S9A) and decreased the
336 methylation levels of 5mC and 5hmC in oocytes (Fig. 4B-D). These
337 findings indicate that melatonin may regulate the re-methylation process in
338 oocytes.
339 To confirm whether melatonin regulates methylation in oocytes via the
340 cAMP pathway, we examined the expression of ADCYs in oocytes using
341 RT-PCR, and found that ADCY5, 6, and 9 were expressed in oocytes (Fig.
342 S9B). The melatonin antagonist luzindole significantly increased the
343 expression of ADCY6 and ADCY9 in oocytes, and melatonin reduced the
344 expression of ADCY6 (Fig. 4E). However, the expression of ADCY5 was
345 lower in the luzindole and melatonin groups compared with the control
346 (Fig. 4E). In addition, the melatonin antagonist luzindole increased, while
347 melatonin decreased the concentration of cAMP in oocytes, respectively
348 (Fig. 4F). These results suggest that melatonin may regulate the synthesis
349 of cAMP via ADCY6 in oocytes. To further confirm the role of cAMP in
350 regulating the methylation of oocytes, we treated mice with SQ22536, an

351 inhibitor of ADCYs, and found that this treatment significantly reduced the
352 global methylation of 5mC and the concentration of cAMP in oocytes
353 (n≥51 Fig. 5A-C). Whereas, the ADCYs activator forskolin significantly
354 increased the cAMP concentration and global methylation of 5mC in
355 oocytes (Fig. 5A-C). 8-Bromo-cAMP, a cAMP analogue, also increased
356 the global methylation in oocytes (n≥41 Fig. 5D, E). cAMP functions by
357 activating the downstream protein PKA. When we treated mice with H89
358 2HCL, a PKA antagonist, the global methylation of 5mC was significantly
359 reduced in oocytes (n≥24 Fig. 5F, G). These results suggest that melatonin
360 may mediate the methylation of oocytes via the cAMP/PKA pathway.
361 cAMP activates PKA which further phosphorylates CREB to regulate gene
362 expression. In oocytes, DNA re-methylation is regulated by DNMTs
363 including DNMT3a, DNMT3l, and DNMT1. Therefore, we next
364 investigated whether melatonin regulates DNMTs expression via the
365 cAMP/PKA/CREB pathway in oocytes. We examined the expression of
366 CREB1, CREM (cAMP responsive element modulator), CREB3l2 (cAMP
367 responsive element binding protein 3 like 2), and ATF1 (activating
368 transcription factor 1) in oocytes. Results showed that ADCYs activator
369 forskolin treatment significantly increased the mRNA expression of
370 CREB1 and CREM, and that the expression of CREB3l2 and ATF1 was
371 slightly increased (Fig. 6A). In addition, the ADCYs inhibitor SQ22536
372 significantly reduced the expression of CREB1 and CREB3l2, although the

373 expression of CREM and ATF1 was slightly decreased in oocytes (Fig. 6A).
374 Furthermore, treatment with the ADCYs inhibitor SQ22536 significantly
375 reduced the concentration of pCREB1, but it was increased by forskolin
376 treatment in oocytes (n≥36 Fig. 6B, C). The pCREB1 level was also
377 increased by 8-Bromo-cAMP and decreased by the PKA antagonist H89
378 2HCL in oocytes (n≥28 Fig. 6D-G). These results suggest that the
379 expression and phosphorylation of CREB1 can be regulated by the
380 cAMP/PKA pathway. Yang *et al.* demonstrated that CREB regulated
381 DNMT3a expression in neurons of the dorsal root ganglion by binding to
382 the promoter region (Yang et al., 2021). In the present study, the binding of
383 pCREB1 with relative regions of DNMTs was examined using CUT & Tag
384 assay. Each sample contained 500 GV oocytes, and two replicates were
385 involved. The sequencing result revealed that five fragments including 10
386 pCREB1 binding motifs (predicted using online tool JASPAR, Table S4)
387 were associated with DNMTs, including 3 fragments at intron 1 and distill
388 intergenic regions of DNMT3a, 1 fragment at the promoter region of
389 DNMT1, and 1 fragment at intron 13 of DNMT3l (Table S5). These results
390 suggest that pCREB1 may have contributions to regulate the expression of
391 DNMTs.
392 Next, we investigated the expression of DNMT1, DNMT3a, and DNMT3l
393 in oocytes. The melatonin inhibitor luzindole (slightly) and the ADCYs
394 activator forskolin (significantly) increased the expression of DNMT1 and

395 DNMT3a, respectively (Fig. 7A, B). Melatonin and the ADCYs inhibitor
396 SQ22536 significantly and slightly reduced the expression of DNMT1 and
397 DNMT3a in oocytes, respectively (Fig. 7A, B). The protein level of
398 DNMT3a in GV oocytes was also significantly increased by 8-Bromo-
399 cAMP and decreased by the PKA antagonist H 89 2HCL, respectively
400 (n≥48 Fig. 7C-F). Although DNMT1 is well known as a maintenance
401 methyltransferase, it also contributes to *de novo* methylation in oocytes (Li
402 et al., 2018). Therefore, we examined the localization of DNMT1 in
403 oocytes, and found that 8-Bromo-cAMP treatment significantly increased
404 the localization of DNMT1 in the nucleus of oocytes, but it was reduced
405 by the PKA antagonist H89 2HCL (n≥22 Fig. 7G-J). When the activation
406 of DNMTs was inhibited by 5-azacytidine, the methylation level in GV
407 oocytes was significantly decreased (n≥43 Fig. S10). These results suggest
408 that melatonin may influence the genomic methylation of oocytes via
409 regulating the expression of DNMT1 and DNMT3a mediated via the
410 cAMP/PKA/CREB pathway.

411 **Increased DNMTs mediate hyper-methylation of HFD oocytes via**
412 **cAMP/PKA/CREB pathway**

413 To explore how melatonin regulates the hyper-methylation of HFD oocytes,
414 we examined the expression of DNMTs. Results showed that maternal
415 obesity in mice significantly increased the expression of DNMT1,
416 DNMT3a, and DNMT3l in oocytes (Fig. 8A). Thus, we aimed to confirm

417 whether the cAMP/PKA/CREB pathway mediated the increased
418 expression of DNMTs in HFD oocytes. We examined the concentration of
419 cAMP in oocytes, and found that maternal obesity significantly increased
420 the concentration of cAMP in oocytes compared with that in CD group (Fig.
421 8B). The mRNA expression of CREB1, but not CREM, in the HFD oocytes
422 was significantly increased compared with that in CD group (Fig. 8C), and
423 the pCREB1 level in HFD oocytes was also significantly increased (n≥49
424 Fig. 8D, E). However, the increased level of pCREB1 was reduced by
425 exogenous melatonin treatment (Fig. 8D, E). When obese females were
426 treated with the PKA antagonist H89 2HCL, both 5mC and pCREB1 levels
427 were significantly reduced in oocytes (n≥17 Fig. 8F-I). These results
428 suggest that reduced melatonin in obese mice may increase the expression
429 of DNMTs via the cAMP/PKA/CREB pathway.
430 The increased expression of DNMT3a (Fig. 8A) may have contributed to
431 the genomic hyper-methylation of HFD oocytes because the primary
432 function of DNMT3a is *de novo* DNA methylation. The *de novo*
433 methylation function of DNMT1 is usually prevented by *Stella* (also
434 known as *Dppa3* or *PGC7*) in oocytes (Bostick et al., 2007). Nevertheless,
435 maternal obesity significantly reduces the expression of *Stella* in oocytes
436 (Han et al., 2018), which indicates that DNMT1 may also contribute to the
437 hyper-methylation of the HFD oocytes. We found that the localization of
438 DNMT1 in the nuclei of HFD oocyte was significantly increased, which

439 could be reduced by the PKA antagonist H89 2HCL treatment (n≥24 Fig.
440 8J, K). These results suggest that the decreased melatonin induced by
441 maternal obesity increases the expression of DNMTs via the
442 cAMP/PKA/CREB pathway, which results in the hyper-methylation in
443 HFD oocytes.

444 **Discussion**

445 Maternal obesity has negative effects on oocyte quality and offspring
446 health, but the underlying mechanisms are not well understod. In the
447 present study, we found that maternal obesity induced hyper-methylation
448 in oocytes, and that the abnormal methylation, at least in part, is transmitted
449 to F2 oocytes in females, which may be associated with the occurrence and
450 inheritance of metabolic disorders. Maternal obesity induced metabolic
451 changes in the serum. The decreased melatonin in serum may be involved
452 in regulating the hyper-methylation of HFD oocytes by increasing the
453 expression of DNMTs, which is mediated by the cAMP/PKA/CREB
454 pathway.

455 Transgenerational epigenetic inheritance is common in plants, but related
456 investigations in mammals are hindered by epigenetic reprogramming
457 events during gametogenesis and early embryo development (Schmitz &
458 Ecker, 2012; Xavier, Roman, Aitken, & Nixon, 2019). In mammals,
459 isogenic agouti viable yellow (A^{vy}) and axin-fused ($Axin^{Fu}$) mice, whose
460 phenotypes are regulated by the DNA methylation level of IAP (intra-

461 cisternal A particle long terminal repeat) respectively located at the
462 upstream and in intron 6, are solid evidence confirming the
463 transgenerational inheritance of epigenetic modifications (Morgan,
464 Sutherland, Martin, & Whitelaw, 1999; Rakyan, Blewitt, Druker, Preis, &
465 Whitelaw, 2002). Nevertheless, epigenetic modifications can be affected
466 by environmental factors such as metabolic diseases and diet. The
467 intergenerational inheritance of phenotypes and epigenetic changes
468 induced by maternal environmental factors have been confirmed by
469 previous studies (B. Chen et al., 2022; Ge et al., 2014), but there are still
470 many debates about the transgenerational inheritance of epigenetic changes
471 induced by environment. Rats from stressed mothers are more likely to be
472 stressed, and that can be transmitted across generations, but this
473 transgenerational inheritance is not mediated by gametes (Weaver et al.,
474 2004). Females cannot mediate the transgenerational inheritance of hyper-
475 methylation induced by diet in A^{vy} mice (Robert A. Waterland, Travisano,
476 & Tahiliani, 2007), but another study reported that if the A^{vy} allele is from
477 the father, the hyper-methylation induced by diet during pregnancy can be
478 retained in germ cells (Cropley, Suter, Beckman, & Martin, 2006). Anway
479 *et al.* reported that the abnormal spermatogenesis induced by the exposure
480 of vinclozolin during pregnancy can be transmitted across four generations
481 via sperm (Anway, Cupp, Uzumcu, & Skinner, 2005). We previously
482 reported that maternal obesity disturbed DNA methylation status of

483 imprinted genes in oocytes (Ge et al., 2014), but the transgenerational
484 inheritance was not observed. We also demonstrated that disturbed
485 methylation in oocytes induced by undernourishment in utero could be
486 inherited, at least partly, by F2 oocytes via females (S.-B. Tang et al., 2023).
487 Recently, Takahashi *et al.* edited DNA methylation of promoter-associated
488 CGIs, and found that the edited DNA methylation, associated with
489 disrupted metabolism, was stably inherited by multiple generations
490 (Takahashi et al., 2023). In the present study, we found that maternal
491 obesity induced genomic hyper-methylation in oocytes, and that a part of
492 the abnormal methylation was transmitted to F2 via female gametes.
493 Moreover, the transmission of metabolic disorders has also been observed
494 across two generations. These results suggest that the transgenerational
495 inheritance of abnormal methylation induced by maternal obesity, at least
496 in part, can be mediated by oocytes, which may be a reason for the
497 inheritance of metabolic disorders.
498 During the methylation process, the methyl group is donated by SAM
499 which is generated from homocysteine, 5-methyltetrahydrofolate
500 (5mTHF), and methionine. 5mTHF is an intermediate of one-carbon
501 metabolism (Mentch & Locasale, 2016). One-carbon units such as folate
502 and vitamin B12 are crucial for the establishment of methylation (Mentch
503 & Locasale, 2016). Disturbed glucose and lipid metabolism also has a
504 negative influence on DNA methylation (Keller et al., 2014). These

505 indicate that abnormal metabolism induced by maternal obesity (King,
506 2006) may play a key role in the genomic hyper-methylation in oocytes. In
507 the present study, we found that the metabolomics of serum from HFD
508 mice was distinguishable from that of serum from CD mice. Although the
509 concentrations of vitamin B6 and methionine were higher in HFD serum
510 than that in CD, this may not be an important reason for the genomic hyper-
511 methylation in oocytes because the concentrations of SAM, SAH, and
512 HCY in the livers and oocytes was similar between CD and HFD mice. In
513 humans, obesity reduces the melatonin level in circulation (Overberg et al.,
514 2022; Virto et al., 2018). In the present study, we also found that maternal
515 obesity induced by high-fat diet reduced the concentration of melatonin in
516 the serum. Melatonin not only can decrease body weight, but also regulates
517 DNA methylation of somatic cells and germ cells (Davoodvandi et al.,
518 2022; Lan et al., 2018). Nevertheless, the molecular mechanism by which
519 melatonin regulates DNA methylation in oocytes is still unclear. Melatonin
520 has two receptors, MT1 and MT2, both of which have been identified in
521 oocytes (Wang et al., 2021). Melatonin receptors interact with the inhibitor
522 G-protein and can regulate gene expression via the cAMP/PKA/CREB
523 pathway (Wongprayoon & Govitrapong, 2021). CREM and cAMP mediate
524 DNA methylation in somatic cells by regulating the expression of *DNMT3a*
525 (Fang et al., 2015; Hedrich et al., 2014). In neurons, CREB interacts with
526 the promoter of *DNMT3a* to regulate its expression and DNA methylation

527 (Yang et al., 2021). In the present study, we found that melatonin, which is
528 mediated by the cAMP/PKA/CREB pathway, regulates methylation in
529 oocytes by increasing the expression of DNMT1 and DNMT3a. Similar
530 results were also observed in HFD oocytes. Hyper-methylation of HFD
531 oocytes can be reduced by exogenous melatonin and PKA inhibitors. These
532 suggest that decreased melatonin levels are involved in regulating the
533 genomic hyper-methylation of HFD oocytes by increasing the expression
534 of DNMTs, which is mediated by the cAMP/PKA/CREB pathway.
535 During follicular development, re-methylation in oocytes is catalyzed
536 mainly by DNMT3a and DNMT3l (Kibe et al., 2021). DNMT1 is usually
537 responsible for maintaining DNA methylation, but DNMT1 also
538 contributes to CG methylation in oocytes (Shirane et al., 2013). During
539 normal oocyte development, DNMT1 is mainly prevented from the nuclei
540 by *Stella*. When the *Stella* level is knocked out, *Uhrf1* (Ubiquitin-like
541 containing PHD Ring Finger 1) moves to the nucleus from the cytoplasm
542 and recruits DNMT1 to chromatin, resulting in hyper-methylation (Li et al.,
543 2018). Maternal obesity significantly deceases the expression of *Stella* in
544 oocytes (Han et al., 2018). These suggest that maternal obesity may induce
545 hyper-methylation in oocytes. In the present study, we found that maternal
546 obesity increased the genomic DNA methylation of GV and MII oocytes,
547 the expression of DNMT1 and its localization at chromatin in GV oocytes.
548 These suggest that reduced *Stella* in HFD oocytes may recruit more

549 DNMT1 into chromatin resulting in hyper-methylation. Nevertheless, Han
550 LS *et al.* reported that maternal obesity has no significant influence on
551 whole genome methylation of GV oocytes and Hou YJ *et al.* reported that
552 maternal obesity reduces whole genome methylation of NSN (no Hoechst-
553 positive rim surrounding the nucleolus) GV oocytes. This contradiction
554 may be associated with the methods used to examine the methylation level
555 and the sample size.
556 In summary, we found that maternal obesity induced genomic hyper-
557 methylation in oocytes and that at least a part of the altered methylation
558 can be transmitted to F2 oocytes, which may be a reason for the inheritance
559 of metabolic disorders. Furthermore, reduced melatonin in HFD mice was
560 involved in regulating the genomic hyper-methylation of oocytes by
561 increasing the expression of DNMTs, and this process was mediated by the
562 cAMP/PKA/CREB pathway. However, there are some limitations for the
563 present study: there is not enough evidence to confirm the role of altered
564 DNA methylation in metabolic disorders in the offspring of obese mothers
565 The molecular mechanisms by which DNA methylation escapes
566 reprogramming in oogenesis have not been elucidated. There are may be
567 other mechanisms involved in regulating genomic hyper-methylation in
568 HFD oocytes. Therefore, more studies are needed in the short future.

569 **Materials and methods**

570 **Mice**

571 C57BL/6 mice were purchased from Jinan Pengyue Company (Jinan,
572 China). Mice were housed in the controlled room with 12 h light and 12 h
573 dark cycle, and at 23-25℃. The Animal Ethics Committee of Qingdao
574 Agricultural University supported all procedures (QAU201900326).
575 For the obesity model, female C57BL/6 mice at the age of 4 weeks were
576 randomly divided into two groups fed with high-fat diet (HFD, Research
577 Diets, D12492, USA) and normal diet (CD) for 12 weeks, respectively. We
578 examined the body weight every week. The formulation of the diets is
579 presented in Table S6.
580 Offspring were produced according to the schedule in Fig.1J. For F1
581 offspring, female HFD and CD mice were mated with normal adult male
582 C57BL/6 mice, respectively, and the offspring were marked as HF1 and
583 CF1. To avoid the effects of males on methylation, the same males were
584 used to produce F2: female HF1 and CF1 mating with normal males,
585 marked as HF2 and CF2.
586 **Immunofluorescence**
587 Briefly, oocytes were fixed with 4% PFA (paraformaldehyde),
588 permeabilized with 0.5% TritonX-100, and blocked with 1% BSA (bovine
589 serum albumin). After that, the oocytes were incubated with primary
590 antibodies overnight at 4℃. The secondary antibodies were stained for 1 h
591 at room temperature. For 5mC and 5hmC staining, the oocytes were treated
592 with 4 N HCl for 10 min after permeabilization, and then transferred into

593 100mM Tris-HCl for 10 min. After washed 3 times using PBS/BSA with
594 0.05% Tween 20, the oocytes were blocked with PBS/BSA for 1 h, and
595 incubated with primary antibodies overnight at 4℃. Secondary antibodies
596 were stained for 1 h at room temperature. Then, oocytes were transferred
597 into DAPI with mounting and sealed. Fluorescence signal was examined
598 using a laser scanning confocal microscope (Leica SP5, Germany). The
599 relative fluorescence intensity was examined using Image J.

600 **Antibodies**

601 Primary antibodies used in the present study included anti-5mC antibody
602 (Abcam, ab73938), anti-5hmC antibody (Abcam, ab214728), anti-pCREB
603 antibody (Cell Signaling Technology, 9198S), anti-DNMT3a antibody
604 (Active motif, 61478), and anti-DNMT1 antibody (Active motif, 39204).

605 **Whole-genome bisulfite sequencing and analysis**

606 Metaphase II (MII) oocytes were collected from the oviduct. For each
607 sample, 100 oocytes from at least 10 mice were pooled together and
608 transferred to lysis buffer. Genomic DNA was fragmented, and the end was
609 repaired. Then, fragmentations were ligated with adapters. Bisulfite
610 treatment was performed using EZ DNA Methylation-Direct (Zymo
611 Research). Lambda DNA was used as a control. After that, the sequencing
612 library was established and sequenced using Illumina HiSeq/NovaSeq
613 (Novogene, China). The raw data quality was evaluated using FastQC, and
614 low quality data and adapters were trimmed using fastp. Clean data were

615 compared to the reference genome mm10. Methylated C site calling was
616 performed using Bismark. Differentially methylated regions (DMRs) were
617 identified using DSS-single. The enrichment of genes in the KEGG
618 pathway was carried out using the online tool KOBAS.

619 **qPCR**

620 Total RNA was extracted from oocytes or tissues using RNAprep Pure
621 Micro Kit (Tiangen, DP420) or RNA Easy Fast Kit (Tiangen, DP451).
622 cDNA was synthesized using Hifair III 1st Strand cDNA Synthesis Kit
623 (Yeasen, China). cDNA was used as templates to examined the relative
624 expression of genes. Housekeeping genes *Ppia* and *Gapdh* were used as
625 references. Relative expression was calculated as $2^{-\Delta\Delta Ct}$.

626 **Bisulfite sequencing (BS)**

627 Each sample included 5 oocytes and at least 20 samples were used for each
628 DMR. The samples were treated as described in a previous study (Ge et al.,
629 2014). Briefly, samples were treated with lysis buffer and 0.3 M NaOH,
630 respectively. After that, samples were embedded in 2% low melting point
631 agarose (Sigma), which was treated with fresh bisulfite solution (2.5 M
632 sodium metabisulfite, Merck; 125 mM hydroquinone, Sigma; pH 5) for 4
633 h. Treated DNA was used as templates to amplify the target fragment using
634 nest-PCR. PCR products were cloned to T-vector and sequenced.
635 Methylation status was analyzed using BiqAnalyzer, which can remove the

636 low conversion rate (<97%) and possible repeat sequences. At least 10
637 available clones was used for each DMR.

638 **Glucose and insulin tolerance**

639 Glucose and insulin tolerance (GTT and ITT) were examined as previously
640 reported (S. B. Tang et al., 2023). Briefly, mice were treated with glucose
641 at 2 g/kg body weight or insulin (Actrapid®, Novo Nordisk) at 10 IU/kg
642 body weight after 16 h or 4 h fasting, respectively. After that, blood glucose
643 was measured by tail blood at 0, 30, 60, 90, and 120 min, respectively.

644 **ELISA**

645 Concentrations of cAMP, SAM, SAH, and HCY were examined using
646 ELISA kits (Jinma Biotechnology Co. Ltd, Shanghai, China) according to
647 the handbook. A standard curve was produced using four-parameters
648 logistics.

649 **Non-target metabolomics in serum**

650 Metabolites in the serum were examined using LC-MS/MS (BGI, Wuhan,
651 China). Raw date were treated with Compound Discoverer 3.1 (Thermo
652 Fisher Scientific, USA). After that, preprocessing of the exported data was
653 performed using metaX. Metabolites were identified according to the
654 databases of BMDB (BGI), mzCloud and ChemSpider (HMDB, KEGG,
655 LipidMaps). Identified metabolites were annotated according to KEGG
656 and HMDB. Differential metabolites were scanned using PCA and PLS-
657 DA combined with fold changes and Student's t test.

658 **Chemicals**

659 Inhibitors used in the present study included luzindole (Sigma), SQ22536
660 (Selleck), forskolin (Selleck), H89 2HCL (Selleck), and azacitidine
661 (Selleck). 8-Bromo-cAMP was purchased from Selleck. Melatonin (Sigma)
662 was injected by tail vein for 14 days. The other chemicals were
663 administrated via intraperitoneal injection for 14 days. The control group
664 was injected with the appropriate solutions.

665 **CUT & Tag and sequencing**

666 For each sample, 500 oocytes were pooled together for this experiment,
667 and two replicates were performed. Library was established using
668 Hyperactive® Universal CUT&Tag Assay Kit (Vazyme, China) according
669 to the manufacturer's instructions. Briefly, oocytes were washed with
670 washing buffer and transferred into tubes with ConA Beads Pro for 10 min
671 at room temperature. The tubes were placed on a magnetic rack for 2 min,
672 and then discarded the supernatant. After that, 50 μl of precooled antibody
673 buffer and primary antibody were added and incubated overnight at 4 ℃.
674 Then, tubes were put on a magnetic rack for 2 min, discarded supernatant,
675 and added 50 μl Dig-wash buffer with secondary antibody (1:100) into
676 tubes incubated at room temperature for 60 min. Samples were washed
677 three times, and then incubated with pA/G-Tnp pro for 1 h at room
678 temperature. After washing, 50 μl of TTBL was added to the samples and
679 incubated at 37℃ for 1 h. Then, 2 μl 10% SDS and DNA Spike-in were

680 added to the samples, which were incubated at 55 ℃ for 10 min.
681 Supernatant was transferred into a new tube after being putted on a
682 magnetic rack for 2 min. 25 μl DNA Extract Beads Pro was added into
683 supernatant, incubated 20 min at room temperature, and then washed two
684 times with B&W buffer. After that, the DNA Extract Beads Pro was re-
685 suspended in 15 μl ddH_2O, and amplified at 60℃ for 20 cycles. Library
686 quality was examined using Qubit, AATI, and QPCR, and then sequenced
687 using NovaSeq 6000 (Novogene, China). Adaptor and low-quality reads
688 were removed from the raw data, and clean data were used for further
689 analysis. Reads were mapped to the mouse reference genome mm39 using
690 Bowtie2. Peak calling was performed using MACS2 at q-value <0.05. The
691 peak was subsequently annotated into related gene regions.

692 **Statistical analysis**

693 Average data are presented as mean ± SE (standard error), and the
694 statistical difference was calculated using two-tail independent-samples t
695 test. Methylation level is presented as a percentage, and the statistical
696 difference was calculated using the chi-square test. If p value < 0.05, the
697 statistical difference was considered to be significant.

698 **Acknowledgement**

699 This work was supported by the National Natural Science Foundation of
700 China (31872312), National R&D Program of China (2022YFC2703500),
701 the Breeding Plan of Shandong Provincial Qingchuang Research Team

(Innovation Team of Farm Animal Cloning 012–1622001), and the Doctor Foundation of Qingdao Agricultural University (6631116008).

Conflicts of interest statement

There are no conflicts of interest to declare.

Data availability

The raw data of sequencing are submitted to the database BGI Sub with No. CRA011654.

Anway, M. D., Cupp, A. S., Uzumcu, M., & Skinner, M. K. (2005). Epigenetic Transgenerational Actions of Endocrine Disruptors and Male Fertility. *Science, 308*(5727), 1466-1469. doi:10.1126/science.1108190

Bartakova, V., Pleskacova, A., Kuricova, K., Pacal, L., Dvorakova, V., Belobradkova, J., . . . Kankova, K. (2016). Dysfunctional protection against advanced glycation due to thiamine metabolism abnormalities in gestational diabetes. *Glycoconj J, 33*(4), 591-598. Retrieved from https://www.ncbi.nlm.nih.gov/pubmed/27287225. doi:10.1007/s10719-016-9688-9

Bostick, M., Kim, J. K., Esteve, P. O., Clark, A., Pradhan, S., & Jacobsen, S. E. (2007). UHRF1 plays a role in maintaining DNA methylation in mammalian cells. *Science, 317*(5845), 1760-1764. Retrieved from https://www.ncbi.nlm.nih.gov/pubmed/17673620. doi:10.1126/science.1147939

Broughton, D. E., & Moley, K. H. (2017). Obesity and female infertility: potential mediators of obesity's impact. *Fertil Steril, 107*(4), 840-847. Retrieved from https://www.ncbi.nlm.nih.gov/pubmed/28292619. doi:10.1016/j.fertnstert.2017.01.017

Chen, B., Du, Y. R., Zhu, H., Sun, M. L., Wang, C., Cheng, Y., . . . Huang, H. (2022). Maternal inheritance of glucose intolerance via oocyte TET3 insufficiency. *Nature, 605*(7911), 761-766. Retrieved from https://www.ncbi.nlm.nih.gov/pubmed/35585240. doi:10.1038/s41586-022-04756-4

Chen, D. H., Wu, K. T., Hung, C. J., Hsieh, M., & Li, C. (2004). Effects of adenosine dialdehyde treatment on in vitro and in vivo stable protein methylation in HeLa cells. *J Biochem, 136*(3), 371-376. Retrieved from https://www.ncbi.nlm.nih.gov/pubmed/15598895. doi:10.1093/jb/mvh131

Chen, X., Xiao, Z., Cai, Y., Huang, L., & Chen, C. (2022). Hypothalamic mechanisms of obesity-associated disturbance of hypothalamic-pituitary-ovarian axis. *Trends Endocrinol Metab, 33*(3), 206-217. Retrieved from https://www.ncbi.nlm.nih.gov/pubmed/35063326. doi:10.1016/j.tem.2021.12.004

Cropley, J. E., Suter, C. M., Beckman, K. B., & Martin, D. I. K. (2006). Germ-line epigenetic modification of the murine Avy allele by nutritional supplementation. *Proceedings of the National Academy of Sciences, 103*(46), 17308-17312. doi:10.1073/pnas.0607090103

Davoodvandi, A., Nikfar, B., Reiter, R. J., & Asemi, Z. (2022). Melatonin and cancer suppression:

739 insights into its effects on DNA methylation. *Cell Mol Biol Lett, 27*(1), 73. Retrieved from
740 https://www.ncbi.nlm.nih.gov/pubmed/36064311. doi:10.1186/s11658-022-00375-z
741 Fang, X., Robinson, J., Wang-Hu, J., Jiang, L., Freeman, D. A., Rivkees, S. A., & Wendler, C. C. (2015).
742 cAMP induces hypertrophy and alters DNA methylation in HL-1 cardiomyocytes. *Am J*
743 *Physiol Cell Physiol, 309*(6), C425-436. Retrieved from
744 https://www.ncbi.nlm.nih.gov/pubmed/26224577. doi:10.1152/ajpcell.00058.2015
745 Ge, Z. J., Luo, S. M., Lin, F., Liang, Q. X., Huang, L., Wei, Y. C., . . . Sun, Q. Y. (2014). DNA methylation
746 in oocytes and liver of female mice and their offspring: effects of high-fat-diet-induced
747 obesity. *Environ Health Perspect, 122*(2), 159-164. Retrieved from
748 https://www.ncbi.nlm.nih.gov/pubmed/24316659. doi:10.1289/ehp.1307047
749 Godfrey, K. M., Reynolds, R. M., Prescott, S. L., Nyirenda, M., Jaddoe, V. W., Eriksson, J. G., &
750 Broekman, B. F. (2017). Influence of maternal obesity on the long-term health of offspring.
751 *Lancet Diabetes Endocrinol, 5*(1), 53-64. Retrieved from
752 https://www.ncbi.nlm.nih.gov/pubmed/27743978. doi:10.1016/S2213-8587(16)30107-3
753 Guan, Q., Wang, Z., Cao, J., Dong, Y., & Chen, Y. (2021). Mechanisms of Melatonin in Obesity: A
754 Review. *Int J Mol Sci, 23*(1). Retrieved from
755 https://www.ncbi.nlm.nih.gov/pubmed/35008644. doi:10.3390/ijms23010218
756 Han, L., Ren, C., Li, L., Li, X., Ge, J., Wang, H., . . . Wang, Q. (2018). Embryonic defects induced by
757 maternal obesity in mice derive from Stella insufficiency in oocytes. *Nat Genet, 50*(3), 432-
758 442. Retrieved from https://www.ncbi.nlm.nih.gov/pubmed/29459681.
759 doi:10.1038/s41588-018-0055-6
760 Hedrich, C. M., Crispin, J. C., Rauen, T., Ioannidis, C., Koga, T., Rodriguez Rodriguez, N., . . . Tsokos,
761 G. C. (2014). cAMP responsive element modulator (CREM) alpha mediates chromatin
762 remodeling of CD8 during the generation of CD3+ CD4- CD8- T cells. *J Biol Chem, 289*(4),
763 2361-2370. Retrieved from https://www.ncbi.nlm.nih.gov/pubmed/24297179.
764 doi:10.1074/jbc.M113.523605
765 Hood, V. L., Berger, R., Freedman, R., & Law, A. J. (2019). Transcription of PIK3CD in human brain
766 and schizophrenia: regulation by proinflammatory cytokines. *Hum Mol Genet, 28*(19),
767 3188-3198. Retrieved from https://www.ncbi.nlm.nih.gov/pubmed/31211828.
768 doi:10.1093/hmg/ddz144
769 Jacobsson, J. A., Rask-Andersen, M., Riserus, U., Moschonis, G., Koumpitski, A., Chrousos, G. P., . . .
770 Fredriksson, R. (2012). Genetic variants near the MGAT1 gene are associated with body
771 weight, BMI and fatty acid metabolism among adults and children. *Int J Obes (Lond), 36*(1),
772 119-129. Retrieved from https://www.ncbi.nlm.nih.gov/pubmed/21304485.
773 doi:10.1038/ijo.2011.11
774 Jin, J. X., Sun, J. T., Jiang, C. Q., Cui, H. D., Bian, Y., Lee, S., . . . Liu, Z. H. (2022). Melatonin Regulates
775 Lipid Metabolism in Porcine Cumulus-Oocyte Complexes via the Melatonin Receptor 2.
776 *Antioxidants (Basel), 11*(4). Retrieved from
777 https://www.ncbi.nlm.nih.gov/pubmed/35453372. doi:10.3390/antiox11040687
778 Johansson, A., Marroni, F., Hayward, C., Franklin, C. S., Kirichenko, A. V., Jonasson, I., . . . Consortium,
779 E. (2010). Linkage and genome-wide association analysis of obesity-related phenotypes:
780 association of weight with the MGAT1 gene. *Obesity (Silver Spring), 18*(4), 803-808.
781 Retrieved from https://www.ncbi.nlm.nih.gov/pubmed/19851299.
782 doi:10.1038/oby.2009.359

783 Kang, H., Jo, A., Kim, H., Khang, R., Lee, J. Y., Kim, H., . . . Shin, J. H. (2018). PARIS reprograms
784 glucose metabolism by HIF-1alpha induction in dopaminergic neurodegeneration.
785 *Biochem Biophys Res Commun, 495*(4), 2498-2504. Retrieved from
786 https://www.ncbi.nlm.nih.gov/pubmed/29287724. doi:10.1016/j.bbrc.2017.12.147
787 Keller, M., Kralisch, S., Rohde, K., Schleinitz, D., Dietrich, A., Schon, M. R., . . . Bottcher, Y. (2014).
788 Global DNA methylation levels in human adipose tissue are related to fat distribution and
789 glucose homeostasis. *Diabetologia, 57*(11), 2374-2383. Retrieved from
790 https://www.ncbi.nlm.nih.gov/pubmed/25145546. doi:10.1007/s00125-014-3356-z
791 Kibe, K., Shirane, K., Ohishi, H., Uemura, S., Toh, H., & Sasaki, H. (2021). The DNMT3A PWWP
792 domain is essential for the normal DNA methylation landscape in mouse somatic cells and
793 oocytes. *PLoS Genet, 17*(5), e1009570. Retrieved from
794 https://www.ncbi.nlm.nih.gov/pubmed/34048432. doi:10.1371/journal.pgen.1009570
795 King, J. C. (2006). Maternal obesity, metabolism, and pregnancy outcomes. *Annu Rev Nutr, 26*,
796 271-291. Retrieved from https://www.ncbi.nlm.nih.gov/pubmed/16704347.
797 doi:10.1146/annurev.nutr.24.012003.132249
798 Lan, M., Han, J., Pan, M. H., Wan, X., Pan, Z. N., & Sun, S. C. (2018). Melatonin protects against
799 defects induced by deoxynivalenol during mouse oocyte maturation. *J Pineal Res, 65*(1),
800 e12477. Retrieved from https://www.ncbi.nlm.nih.gov/pubmed/29453798.
801 doi:10.1111/jpi.12477
802 Li, Y., Zhang, Z., Chen, J., Liu, W., Lai, W., Liu, B., . . . Zhu, B. (2018). Stella safeguards the oocyte
803 methylome by preventing de novo methylation mediated by DNMT1. *Nature, 564*(7734),
804 136-140. Retrieved from https://www.ncbi.nlm.nih.gov/pubmed/30487604.
805 doi:10.1038/s41586-018-0751-5
806 Lyon, P., Strippoli, V., Fang, B., & Cimmino, L. (2020). B Vitamins and One-Carbon Metabolism:
807 Implications in Human Health and Disease. *Nutrients, 12*(9). Retrieved from
808 https://www.ncbi.nlm.nih.gov/pubmed/32961717. doi:10.3390/nu12092867
809 Mentch, S. J., & Locasale, J. W. (2016). One-carbon metabolism and epigenetics: understanding
810 the specificity. *Ann N Y Acad Sci, 1363*(1), 91-98. Retrieved from
811 https://www.ncbi.nlm.nih.gov/pubmed/26647078. doi:10.1111/nyas.12956
812 Morgan, H. D., Sutherland, H. G., Martin, D. I., & Whitelaw, E. (1999). Epigenetic inheritance at the
813 agouti locus in the mouse. *Nat Genet, 23*(3), 314-318. Retrieved from
814 https://www.ncbi.nlm.nih.gov/pubmed/10545949. doi:10.1038/15490
815 Overberg, J., Kalveram, L., Keller, T., Krude, H., Kuhnen, P., & Wiegand, S. (2022). Interactions
816 between nocturnal melatonin secretion, metabolism, and sleeping behavior in
817 adolescents with obesity. *Int J Obes (Lond), 46*(5), 1051-1058. Retrieved from
818 https://www.ncbi.nlm.nih.gov/pubmed/35140394. doi:10.1038/s41366-022-01077-4
819 Qu, J., Sun, M., Wang, X., Song, X., He, H., & Huan, Y. (2020). Melatonin Enhances the Development
820 of Porcine Cloned Embryos by Improving DNA Methylation Reprogramming. *Cell*
821 *Reprogram, 22*(3), 156-166. Retrieved from
822 https://www.ncbi.nlm.nih.gov/pubmed/32207988. doi:10.1089/cell.2019.0103
823 Rakyan, V. K., Blewitt, M. E., Druker, R., Preis, J. I., & Whitelaw, E. (2002). Metastable epialleles in
824 mammals. *Trends Genet, 18*(7), 348-351. Retrieved from
825 https://www.ncbi.nlm.nih.gov/pubmed/12127774. doi:10.1016/s0168-9525(02)02709-9
826 Saeedabadi, S., Abazari-Kia, A. H., Rajabi, H., Parivar, K., & Salehi, M. (2018). Melatonin Improves

The Developmental Competence of Goat Oocytes. *Int J Fertil Steril, 12*(2), 157-163. Retrieved from https://www.ncbi.nlm.nih.gov/pubmed/29707934. doi:10.22074/ijfs.2018.5204

Schmitz, R. J., & Ecker, J. R. (2012). Epigenetic and epigenomic variation in Arabidopsis thaliana. *Trends Plant Sci, 17*(3), 149-154. Retrieved from https://www.ncbi.nlm.nih.gov/pubmed/22342533. doi:10.1016/j.tplants.2012.01.001

Shirane, K., Toh, H., Kobayashi, H., Miura, F., Chiba, H., Ito, T., . . . Sasaki, H. (2013). Mouse oocyte methylomes at base resolution reveal genome-wide accumulation of non-CpG methylation and role of DNA methyltransferases. *PLoS Genet, 9*(4), e1003439. Retrieved from https://www.ncbi.nlm.nih.gov/pubmed/23637617. doi:10.1371/journal.pgen.1003439

Shou, L., Pan, F., & Chin, S. (1969). Pancreatic hormones and hepatic methionine adenosyltransferase in the rat. *Proc Soc Exp Biol Med, 131*(3), 1012-1018. Retrieved from https://www.ncbi.nlm.nih.gov/pubmed/5791769. doi:10.3181/00379727-131-34029

Takahashi, Y., Morales Valencia, M., Yu, Y., Ouchi, Y., Takahashi, K., Shokhirev, M. N., . . . Izpisua Belmonte, J. C. (2023). Transgenerational inheritance of acquired epigenetic signatures at CpG islands in mice. *Cell, 186*(4), 715-731 e719. Retrieved from https://www.ncbi.nlm.nih.gov/pubmed/36754048. doi:10.1016/j.cell.2022.12.047

Tang, S.-B., Zhang, T.-T., Yin, S., Shen, W., Luo, S.-M., Zhao, Y., . . . Ge, Z.-J. (2023). Inheritance of perturbed methylation and metabolism caused by uterine malnutrition via oocytes. *BMC Biology, 21*(1). doi:10.1186/s12915-023-01545-x

Tang, S. B., Zhang, T. T., Yin, S., Shen, W., Luo, S. M., Zhao, Y., . . . Ge, Z. J. (2023). Inheritance of perturbed methylation and metabolism caused by uterine malnutrition via oocytes. *BMC Biol, 21*(1), 43. Retrieved from https://www.ncbi.nlm.nih.gov/pubmed/36829148. doi:10.1186/s12915-023-01545-x

Vaccaro, J. A., & Naser, S. A. (2021). The Role of Methyl Donors of the Methionine Cycle in Gastrointestinal Infection and Inflammation. *Healthcare (Basel), 10*(1). Retrieved from https://www.ncbi.nlm.nih.gov/pubmed/35052225. doi:10.3390/healthcare10010061

Virto, L., Haugen, H. J., Fernandez-Mateos, P., Cano, P., Gonzalez, J., Jimenez-Ortega, V., . . . Sanz, M. (2018). Melatonin expression in periodontitis and obesity: An experimental in-vivo investigation. *J Periodontal Res, 53*(5), 825-831. Retrieved from https://www.ncbi.nlm.nih.gov/pubmed/29900537. doi:10.1111/jre.12571

Wang, J., Zhuo, Z., Ma, X., Liu, Y., Xu, J., He, C., . . . Liu, G. (2021). Melatonin Alleviates the Suppressive Effect of Hypoxanthine on Oocyte Nuclear Maturation and Restores Meiosis via the Melatonin Receptor 1 (MT1)-Mediated Pathway. *Front Cell Dev Biol, 9*, 648148. Retrieved from https://www.ncbi.nlm.nih.gov/pubmed/33937242. doi:10.3389/fcell.2021.648148

Waterland, R. A. (2006). Assessing the effects of high methionine intake on DNA methylation. *J Nutr, 136*(6 Suppl), 1706S-1710S. Retrieved from https://www.ncbi.nlm.nih.gov/pubmed/16702343. doi:10.1093/jn/136.6.1706S

Waterland, R. A., Travisano, M., & Tahiliani, K. G. (2007). Diet-induced hypermethylation at agouti viable yellow is not inherited transgenerationally through the female. *The FASEB Journal, 21*(12), 3380-3385. doi:10.1096/fj.07-8229com

Weaver, I. C., Cervoni, N., Champagne, F. A., D'Alessio, A. C., Sharma, S., Seckl, J. R., . . . Meaney,

871 M. J. (2004). Epigenetic programming by maternal behavior. *Nat Neurosci, 7*(8), 847-854.
872 Retrieved from https://www.ncbi.nlm.nih.gov/pubmed/15220929. doi:10.1038/nn1276
873 Wojcik, M., Mac-Marcjanek, K., Wozniak, L. A., Nadel, I., Lewinski, A., & Cypryk, K. (2014). The
874 association of leukocyte phosphatidylinositol 3-kinase delta overexpression with
875 gestational diabetes mellitus (GDM). *Endokrynol Pol, 65*(1), 17-24. Retrieved from
876 https://www.ncbi.nlm.nih.gov/pubmed/24549598. doi:10.5603/EP.2014.0003
877 Wongprayoon, P., & Govitrapong, P. (2021). Melatonin Receptor as a Drug Target for
878 Neuroprotection. *Curr Mol Pharmacol, 14*(2), 150-164. Retrieved from
879 https://www.ncbi.nlm.nih.gov/pubmed/32316905.
880 doi:10.2174/1874467213666200421160835
881 Xavier, M. J., Roman, S. D., Aitken, R. J., & Nixon, B. (2019). Transgenerational inheritance: how
882 impacts to the epigenetic and genetic information of parents affect offspring health. *Hum*
883 *Reprod Update, 25*(5), 518-540. Retrieved from
884 https://www.ncbi.nlm.nih.gov/pubmed/31374565. doi:10.1093/humupd/dmz017
885 Xiao, P., Nie, J., Wang, X., Lu, K., Lu, S., & Liang, X. (2019). Melatonin alleviates the deterioration of
886 oocytes from mice subjected to repeated superovulation. *J Cell Physiol, 234*(8), 13413-
887 13422. Retrieved from https://www.ncbi.nlm.nih.gov/pubmed/30609033.
888 doi:10.1002/jcp.28018
889 Yang, Y., Wen, J., Zheng, B., Wu, S., Mao, Q., Liang, L., . . . Tao, Y. X. (2021). CREB Participates in
890 Paclitaxel-Induced Neuropathic Pain Genesis Through Transcriptional Activation of
891 Dnmt3a in Primary Sensory Neurons. *Neurotherapeutics, 18*(1), 586-600. Retrieved from
892 https://www.ncbi.nlm.nih.gov/pubmed/33051852. doi:10.1007/s13311-020-00931-5

893

894 **Figure legends**

895 **Figure1 Maternal obesity alters the DNA methylation of oocytes.**

896 (A) Methylation levels of 5mC and 5hmC in oocytes (n>30). 5mC, 5-
897 methylcytosine; 5hmC, 5-hydroxymethylcytosine; DAPI, chromatin.
898 (B, C) Relative fluorescence intensity of 5mC and 5hmC in GV oocytes.
899 (D) Genomic methylation level of MII oocytes examined by single-cell
900 whole genome bisulfite sequencing. The control group (CD) has two
901 replicates, and the obesity group (HFD) has three replicates.
902 (E) Average genomic CG methylation level in MII oocytes. CD, control
903 group; HFD, obesity group; ** means p value < 0.01.

904 (F) CG methylation levels at different regions in MII oocytes. CGI, CpG
905 island; utr5, 5' untranslated region; utr3, 3' untranslated region; repeat,
906 repeat sequence.
907 (G) Total differentially methylated regions (DMRs) in oocytes of control
908 and obesity groups. Hyper-DMRs, hypermethylated DMRs; hypo-DMRs,
909 hypomethylated DMRs.
910 (H) Distribution of DMRs on chromosomes in MII oocytes. Outside-to-in:
911 chromosomes, hyper-DMRs, TEs (transcription end regions), and gene,
912 hypo-DMRs.
913 (I) KEGG pathway enrichment of genes with DMRs at the promoter
914 regions, and the top 20 pathways are presented.
915 (J) Schedule of breeding. Female C57BL/6 mice fed with normal (CD) or
916 high-fat diet (HFD) for 12 weeks were marked as F0. F1 was produced by
917 F0 mated with normal males, respectively, and marked as CF1 and HF1;
918 F2 was produced by female F1 mated with normal males and marked as
919 CF2 and HF2, respectively.
920 **Figure 2 Transgenerational inheritance of metabolic disorders and**
921 **altered DNA methylation.**
922 (A-C) Glucose tolerance (GTT) and insulin tolerance ITT) were tested for
923 female F0, F1, and F2, respectively. * $p<0.05$; ** $p<0.01$.
924 (D-F) DMR methylation at the promoter regions of *Bhlha15*, *Mgat1*, *Taok3*,
925 *Tkt*, and *Pid3cd* in F0, F1, and F2 oocytes was respectively examined using

926 bisulfite sequencing. At least 10 available clones from 80-100 oocytes were
927 used to calculate the methylation level. White circle, unmethylated CG;
928 black circle, methylated CG. * $p<0.05$; ** $p<0.01$.
929 (G) Inheritance of altered methylation in different generations was
930 analyzed. * $p<0.05$; ** $p<0.01$.
931 **Figure 3 Maternal obesity alters metabolome of serum.**
932 (A) Principal component analysis in CD and HFD mice.
933 (B) Differential metabolites in HFD serum compared with those in CD
934 group. Red circles, upregulated metabolites; blue circles, downregulated
935 metabolites.
936 (C) The enrichment of differential metabolites was analyzed using KEGG,
937 and the top 10 enrichment terms are presented.
938 (D) Heat map of the top 20 differential metabolites in HFD serum.
939 (E-G) Comparison of the concentrations of pyridoxine, methionine, and
940 tyrosine among the groups. * $p<0.05$; ** $p<0.01$; *** $p<0.001$.
941 (H-J) Concentrations of SAM, SAH and HCY in the livers were examined
942 by ELISA. Ns, there was no statistical significance between groups.
943 (K) The concentration of SAM in oocytes was analyzed using ELISA. **
944 $p<0.01$.
945 (L) Relative concentration of melatonin in the serum. *** $p<0.001$.
946 (M) Genomic DNA methylation in oocytes was examined using
947 immunofluorescence. CD, control group; HFD, obesity group;

948 HFD+melatonin, obese mice were treated with exogenous melatonin for
949 14 days.
950 (N) Relative fluorescence intensity of 5mC was examined using Image J
951 (CD, n=109; HFD, n=104; HFD+melatonin, n=96). * $p<0.05$; *** $p<0.001$.
952 **Figure 4 Melatonin regulates DNA methylation in oocytes.**
953 (A) Schedule of the possible pathway by which melatonin regulates DNA
954 methylation in oocytes. According to previous studies, we predicted that
955 melatonin might regulate DNA methylation in oocytes via the
956 cAMP/PKA/CREB pathway .
957 (B) Effects of melatonin and its inhibitor luzindole on oocyte methylation
958 were examined using immunofluorescence.
959 (C, D) The relative fluorescence intensities of 5mC and 5hmC were
960 analyzed using Image J (5mC: Control, n=81; Luzindole, n=83; Melatonin,
961 n=86. 5hmC: Control, n=64; Luzindole, n=58; Melatonin, n=49). * $p<0.05$;
962 *** $p<0.001$.
963 (E) The effects of melatonin and its inhibitor luzindole on the expression
964 of adenylate cyclase (ADCY) in oocytes were examined by qPCR. *
965 $p<0.05$; ** $p<0.01$.
966 (F) The concentration of cAMP in oocytes was examined by ELISA. *
967 $p<0.05$; ** $p<0.01$.
968 **Figure 5 Role of cAMP in DNA methylation in oocytes.**
969 (A) Female mice were respectively treated with the ADCY inhibitor

970 SQ22536 or activator forskolin. Oocyte methylation was examined using
971 immunofluorescence.
972 (B) The relative intensity of fluorescence in oocytes was analyzed using
973 Image J (Control, n=107; SQ22536, n=51; Forskolin, n=57). ** $p<0.01$;
974 *** $p<0.001$.
975 (C) cAMP concentration in oocytes was examined using ELISA. * $p<0.05$;
976 ** $p<0.01$.
977 (D) Female mice were treated with the cAMP analogue 8-Bromo-cAMP,
978 and oocyte methylation was examined using immunofluorescence. The
979 relative fluorescence intensity of 5mC was analyzed using Image J (E)
980 (Control, n=41; 8-Bromo-cAMP, n=42). ** $p<0.01$.
981 (F, G) Female mice were treated with the PKA (protein kinase A)
982 antagonist H 89 2HCL, and then oocyte methylation was examined using
983 immunofluorescence. The relative fluorescence intensity of 5mC was
984 analyzed using Image J (G) (Control, n=24; H 89 2HCl, n=25). * $p<0.05$.
985 **Figure 6 Effects of cAMP on CREB1.**
986 (A) The mRNA expression of cAMP-response element binding (CREB)
987 proteins in oocytes was examined by qPCR. * $p<0.05$.
988 (B and C) Phosphorylated CREB1 (pCREB1) in oocytes was examined
989 using immunofluorescence, and the relative fluorescence intensity of
990 pCREB1 was examined by Image J (C) (Control, n=36; SQ22536, n=48;
991 Forskolin, n=41). * $p<0.05$; ** $p<0.01$; *** $p<0.001$.

992 (D and E) After treatment with the cAMP analogue 8-Bromo-cAMP,
993 pCREB1 in oocytes was examined using immunofluorescence. The
994 relative fluorescence intensity was analyzed using Image J (E) (Control,
995 n=28; 8-Bromo-cAMP, n=28). *** $p<0.001$.

996 **Figure 7 Role of the melatonin/cAMP/PKA pathway in the expression**
997 **of DNMTs.**

998 (A) The expression levels of DNMT1, DNMT3a and DNMT3l in oocytes
999 were examined using qPCR after the treatment with SQ22536 and
1000 forskolin. * $p<0.05$.

1001 (B) The relative expressions of DNMT1, DNMT3a and DNMT3l in
1002 oocytes were examined using qPCR after the treatment with luzindole and
1003 melatonin. * $p<0.05$.

1004 (C) After 8-Bromo-cAMP treatment, the relative expression of DNMT3a
1005 in oocytes was examined using immunofluorescence and calculated by
1006 Image J (D) (Control, n=54; 8-Bromo-cAMP, n=70). ** $p<0.01$.

1007 (E and F) Treatment with the PKA antagonist H 89 2HCL treatment
1008 significantly reduced the level of DNMT3a in oocytes examined using
1009 immunofluorescence (Control, n=62; H 89 2HCl, n=48). ** $p<0.01$.

1010 (G and H) DNMT1 localization in the oocyte nucleus was examined using
1011 immunofluorescence after 8-Bromo-cAMP treatment (Control, n=30; 8-
1012 Bromo-cAMP, n=31). *** $p<0.001$.

1013 (I and J) The localization of DNMT1 in oocyte nucleus was reduced by the

1014 treatment with the PKA antagonist H 89 2HCL (Control, n=22; H 89 2HCl,
1015 n=28). ** p<0.01.

1016 **Figure 8 Melatonin regulates DNMTs expression via**
1017 **cAMP/PKA/CREB pathway in HFD oocytes.**

1018 (A) The relative expression of DNMT1, DNMT3a, and DNMT3l in HFD
1019 oocytes was examined using qPCR. * p<0.05; ** p<0.01.

1020 (B) The concentration of cAMP in HFD oocytes was examined using
1021 ELISA. ** p<0.01.

1022 (C) The relative expressions CREB1 and CREM in HFD oocytes were
1023 tested using qPCR. * p<0.05; ** p<0.01.

1024 (D and E) The level of pCREB1 in oocytes was examined using
1025 immunofluorescence, and the relative fluorescence intensity was
1026 calculated by Image J (E) (CD, n=69; HFD, n=49; HFD+melatonin, n=61).
1027 HFD, oocytes from obese mice; CD, oocytes from control mice; HFD +
1028 melatonin, oocytes from obese mice treated with exogenous melatonin. *
1029 p<0.05; *** p<0.001.

1030 (F and G) Treatment with the PKA antagonist H89 2HCL reduced the
1031 methylation level of HFD oocytes (CD, n=48; HFD, n=31; HFD+H 89
1032 2HCl, n=27). ** p<0.01; *** p<0.001.

1033 (H and I) The level of pCREB1 in HFD oocytes was also decreased by the
1034 treatment with the PKA antagonist H89 2HCL (CD, n=17; HFD, n=17;
1035 HFD+H 89 2HCl, n=22). * p<0.05; ** p<0.01; ns, no statistical

1036 significance between groups.

1037 (J and K) Treatment with the PKA antagonist H89 2HCL reduced the

1038 localization of DNMT1 in HFD oocytes (CD, n=24; HFD, n=29; HFD+H

1039 89 2HCl, n=25). ** $p<0.01$; *** $p<0.001$; ns, no statistical significance

1040 between groups.

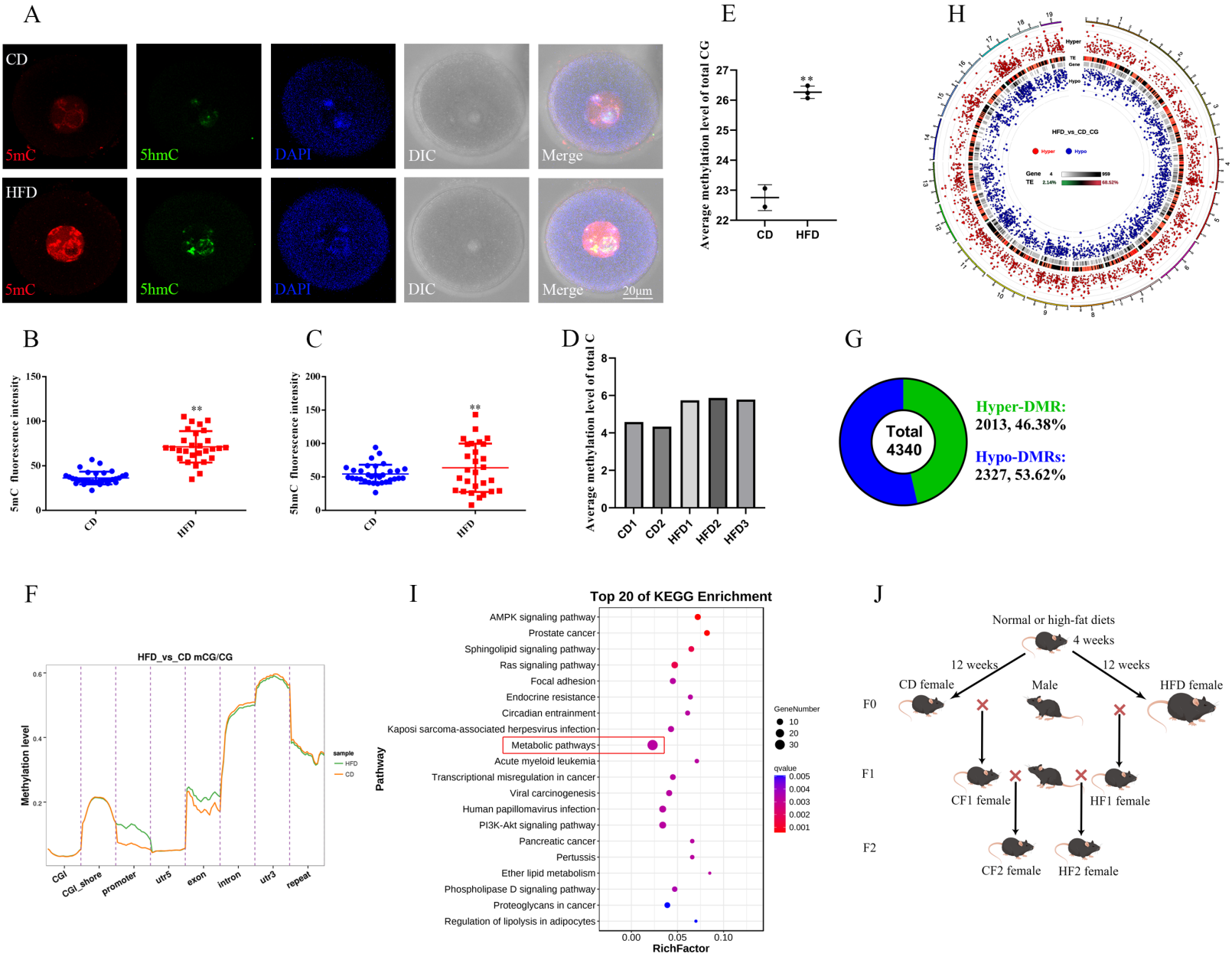
A
CD
5mC
5hmC
DAPI
DIC
Merge
HFD
20μm
E
Average methylation level of total CG
CD
HFD
H
HFD_vs_CD_CG
Hyper
Hypo
Gene
TE
B
5mC fluorescence intensity
CD
HFD
C
5hmC fluorescence intensity
D
Average methylation level of total C
CD1
CD2
HFD1
HFD2
HFD3
G
Total
4340
Hyper-DMR:
2013, 46.38%
Hypo-DMRs:
2327, 53.62%
F
HFD_vs_CD mCG/CG
Methylation level
sample
HFD
CD
CGI
CGI_shore
promoter
utr5
exon
intron
utr3
repeat
I
Top 20 of KEGG Enrichment
AMPK signaling pathway
Prostate cancer
Sphingolipid signaling pathway
Ras signaling pathway
Focal adhesion
Endocrine resistance
Circadian entrainment
Kaposi sarcoma-associated herpesvirus infection
Metabolic pathways
Acute myeloid leukemia
Transcriptional misregulation in cancer
Viral carcinogenesis
Human papillomavirus infection
PI3K-Akt signaling pathway
Pancreatic cancer
Pertussis
Ether lipid metabolism
Phospholipase D signaling pathway
Proteoglycans in cancer
Regulation of lipolysis in adipocytes
Pathway
RichFactor
GeneNumber
qvalue
J
Normal or high-fat diets
4 weeks
12 weeks
12 weeks
CD female
Male
HFD female
F0
F1
F2
CF1 female
HF1 female
CF2 female
HF2 female

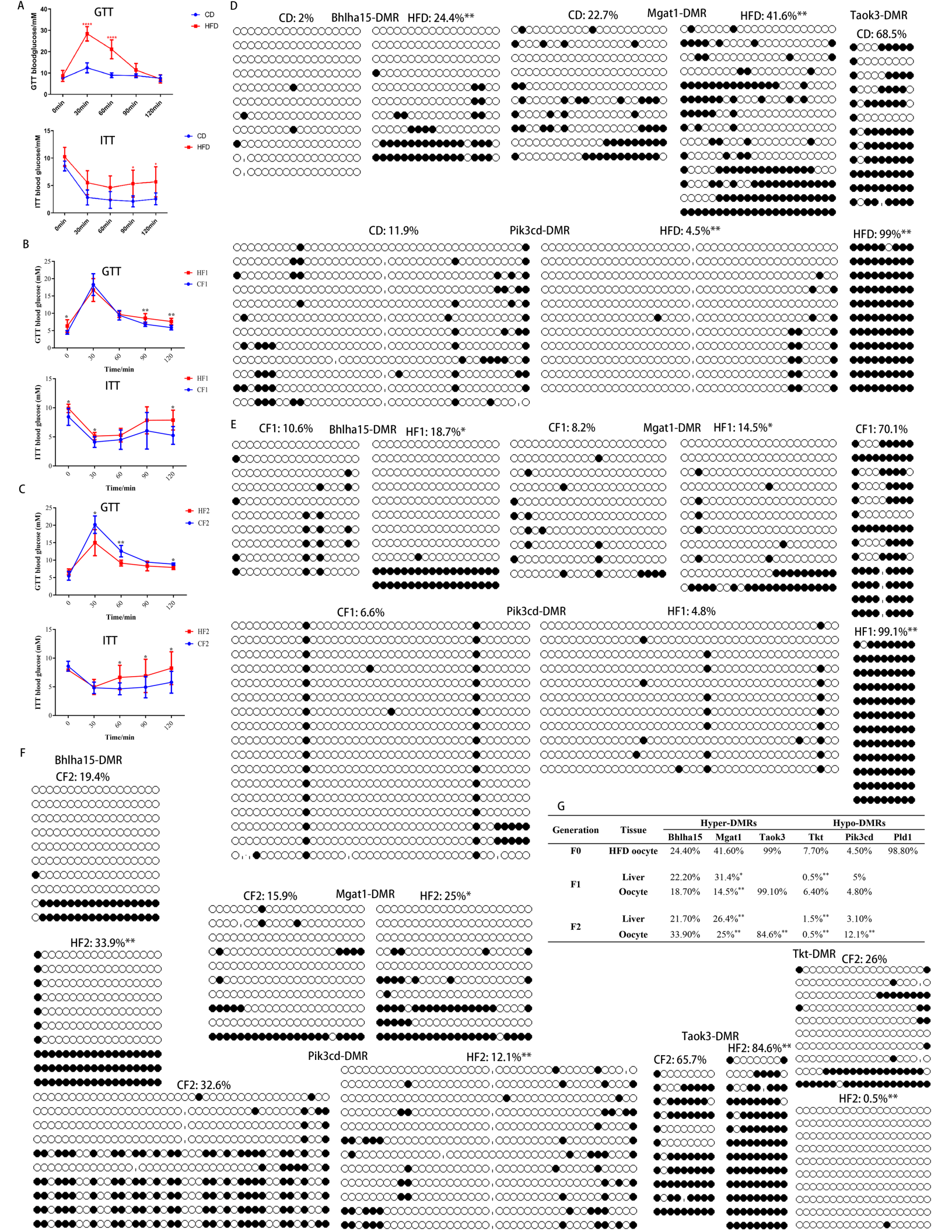

G

Generation	Tissue	Hyper-DMRs			Hypo-DMRs		
		Bhlha15	Mgat1	Taok3	Tkt	Pik3cd	Pld1
F0	HFD oocyte	24.40%	41.60%	99%	7.70%	4.50%	98.80%
F1	Liver	22.20%	31.4%*		0.5%**	5%	
	Oocyte	18.70%	14.5%**	99.10%	6.40%	4.80%	
F2	Liver	21.70%	26.4%**		1.5%**	3.10%	
	Oocyte	33.90%	25%**	84.6%**	0.5%**	12.1%**	

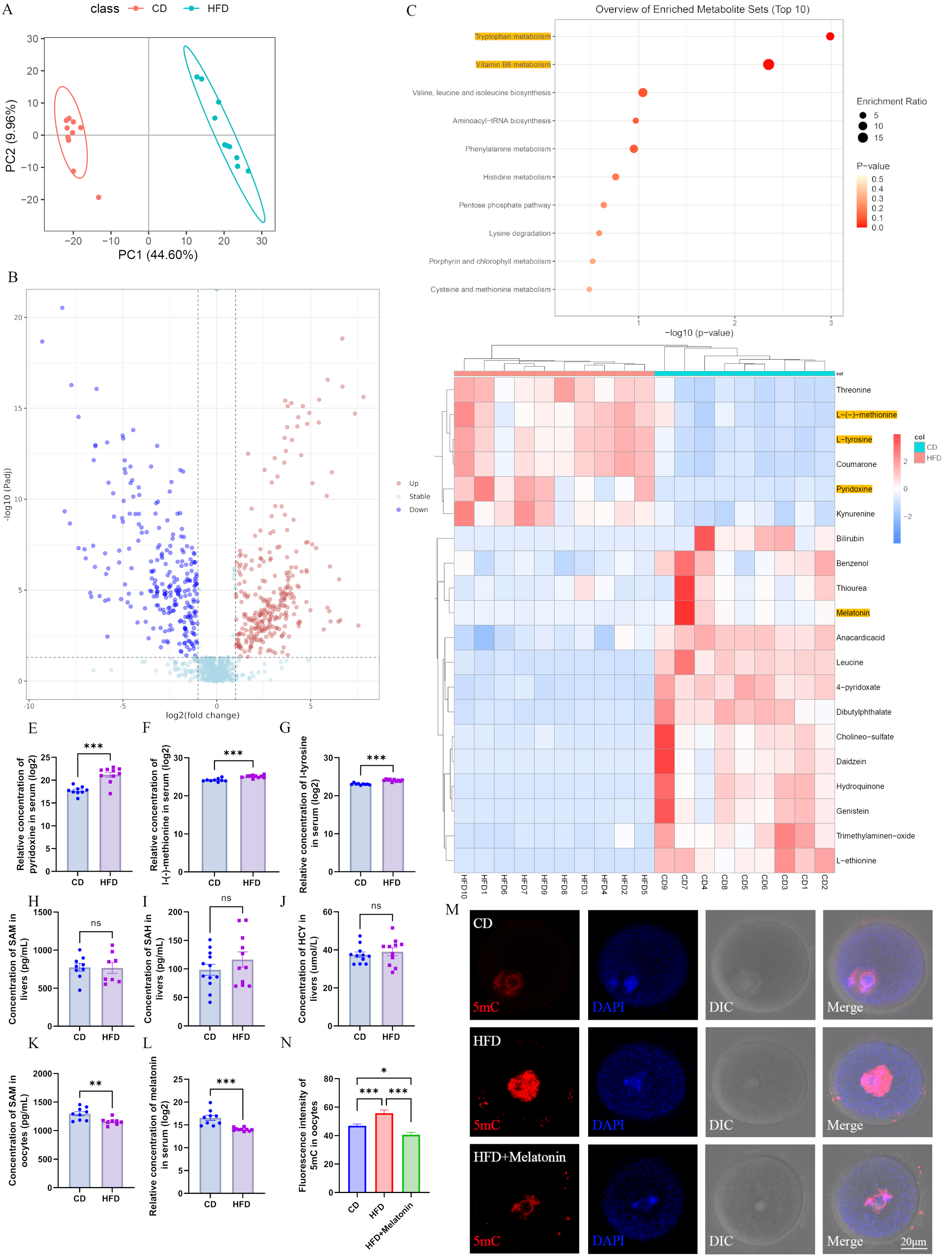
A
class CD HFD
PC2 (9.96%)
PC1 (44.60%)
B
-log10 (Padj)
log2(fold change)
Up
Stable
Down
C
Overview of Enriched Metabolite Sets (Top 10)
Tryptophan metabolism
Vitamin B6 metabolism
Valine, leucine and isoleucine biosynthesis
Aminoacyl-tRNA biosynthesis
Phenylalanine metabolism
Histidine metabolism
Pentose phosphate pathway
Lysine degradation
Porphyrin and chlorophyll metabolism
Cysteine and methionine metabolism
-log10 (p-value)
Enrichment Ratio
P-value
Threonine
L-(-)-methionine
L-tyrosine
Coumarone
Pyridoxine
Kynurenine
Bilirubin
Benzenol
Thiourea
Melatonin
Anacardicacid
Leucine
4-pyridoxate
Dibutylphthalate
Cholineo-sulfate
Daidzein
Hydroquinone
Genistein
Trimethylaminen-oxide
L-ethionine
col
CD
HFD
E
Relative concentration of pyridoxine in serum (log2)
F
Relative concentration of l-(-)-methionine in serum (log2)
G
Relative concentration of l-tyrosine in serum (log2)
H
Concentration of SAM in livers (pg/mL)
I
Concentration of SAH in livers (pg/mL)
J
Concentration of HCY in livers (umol/L)
K
Concentration of SAM in oocytes (pg/mL)
L
Relative concentration of melatonin in serum (log2)
N
Fluorescence intensity of 5mC in oocytes
HFD+Melatonin
M
5mC
DAPI
DIC
Merge
20μm

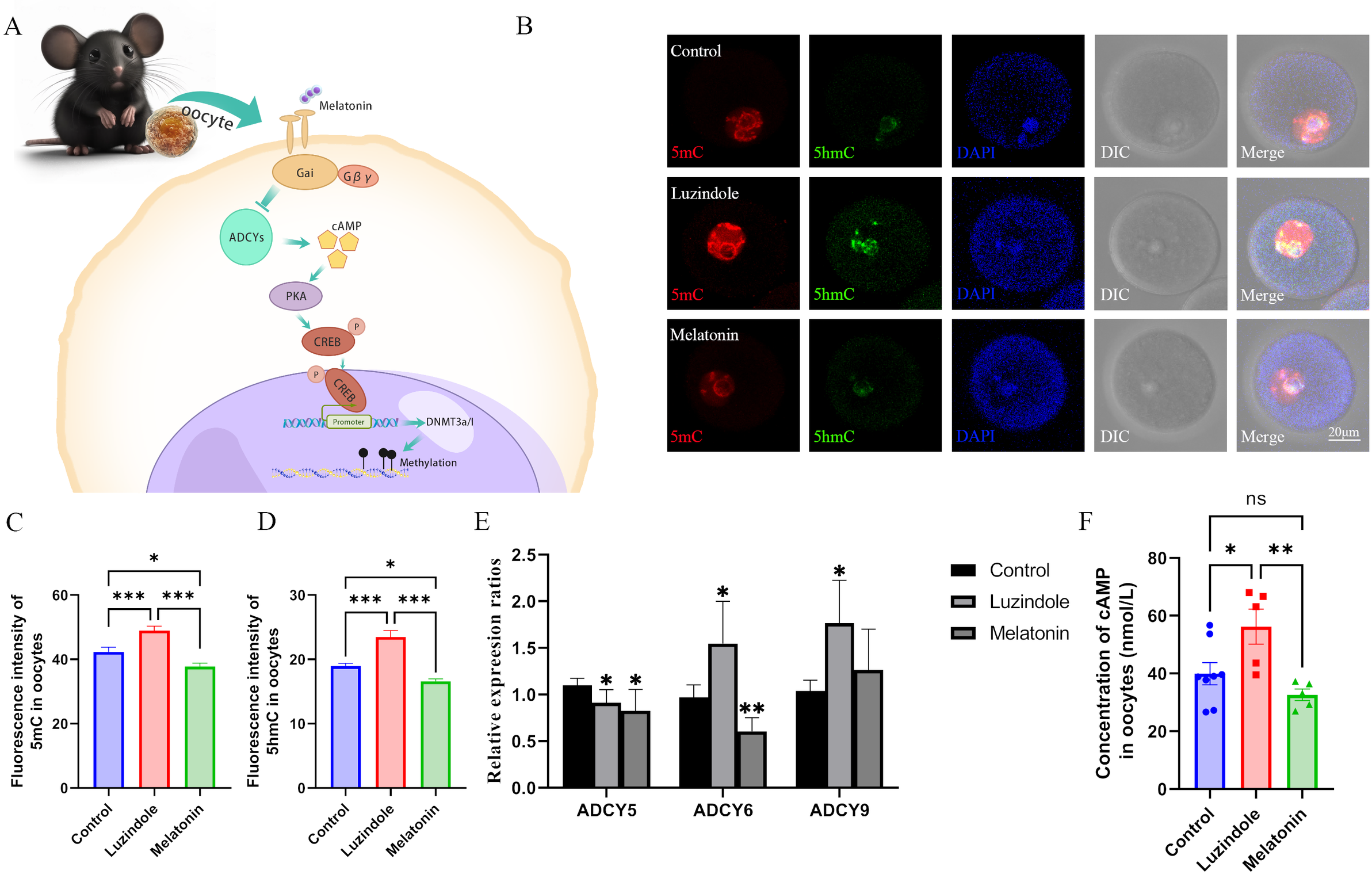
A
B
Oocyte
Melatonin
Gai
Gβγ
ADCYs
cAMP
PKA
CREB
P
CREB
Promoter
DNMT3a/l
Methylation
Control
Luzindole
Melatonin
5mC
5hmC
DAPI
DIC
Merge
20μm
C
Fluorescence intensity of 5mC in oocytes
D
Fluorescence intensity of 5hmC in oocytes
E
Relative expreesion ratios
ADCY5
ADCY6
ADCY9
F
Concentration of cAMP in oocytes (nmol/L)
ns

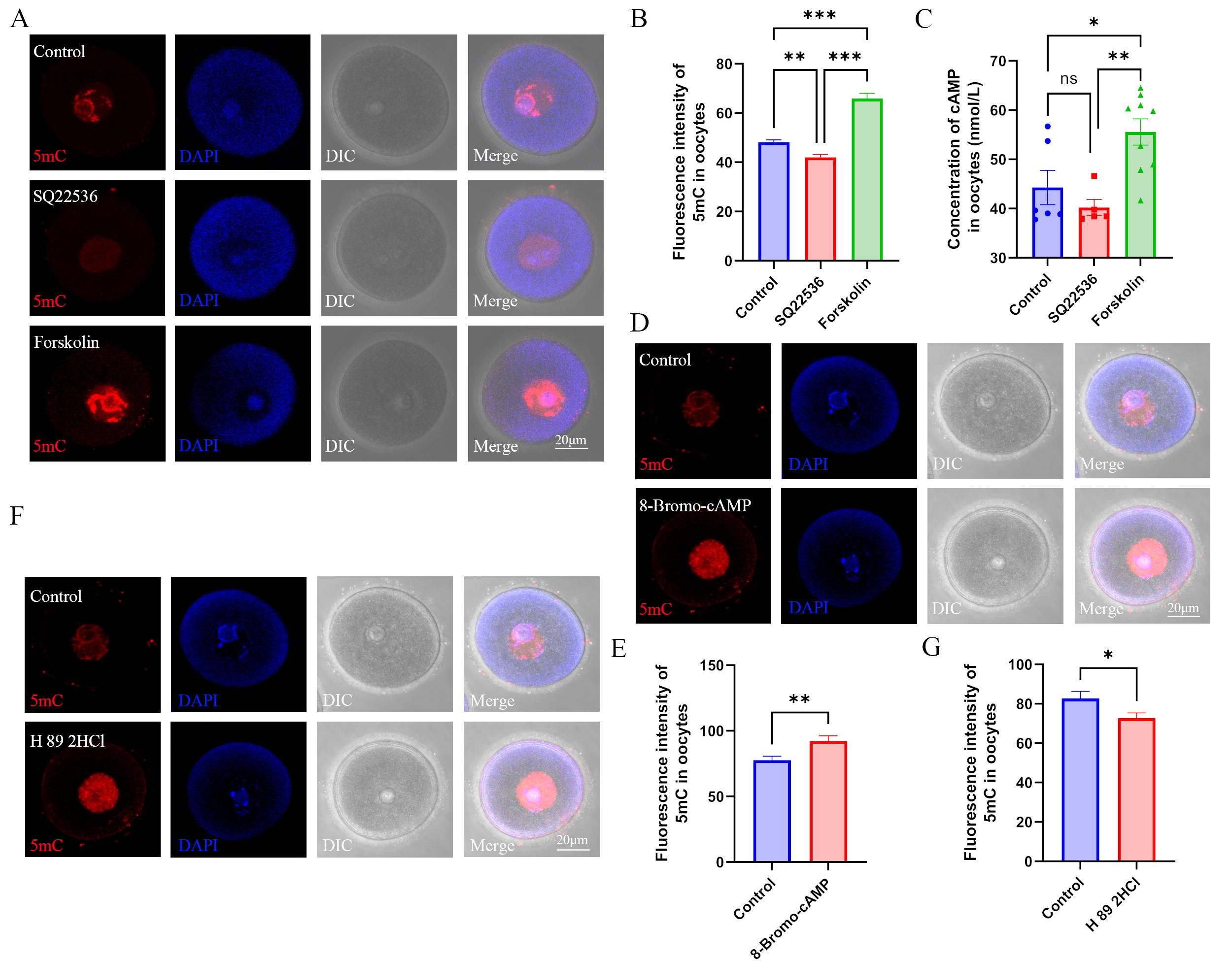
A
Control
SQ22536
Forskolin
5mC
DAPI
DIC
Merge
20μm
B
Fluorescence intensity of 5mC in oocytes
0
20
40
60
80
***
**
***
Control
SQ22536
Forskolin
C
Concentration of cAMP in oocytes (nmol/L)
30
40
50
60
70
*
ns
**
Control
SQ22536
Forskolin
D
Control
8-Bromo-cAMP
5mC
DAPI
DIC
Merge
20μm
E
Fluorescence intensity of 5mC in oocytes
0
50
100
150
**
Control
8-Bromo-cAMP
F
Control
H 89 2HCl
5mC
DAPI
DIC
Merge
20μm
G
Fluorescence intensity of 5mC in oocytes
0
20
40
60
80
100
*
Control
H 89 2HCl

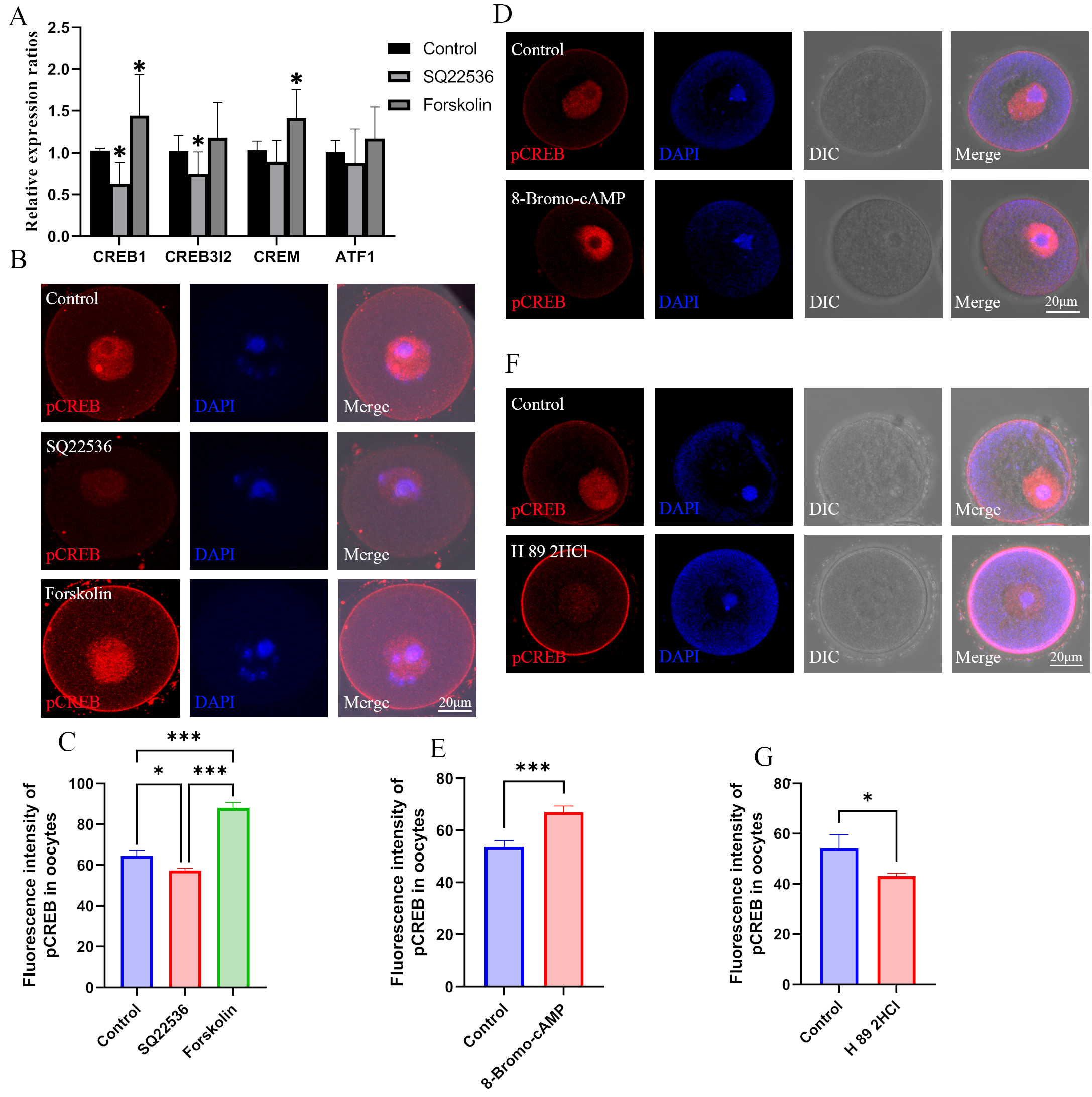
A
Relative expression ratios
2.5
2.0
1.5
1.0
0.5
0.0
Control
SQ22536
Forskolin
CREB1
CREB3I2
CREM
ATF1
B
Control
SQ22536
Forskolin
pCREB
DAPI
Merge
20μm
C
Fluorescence intensity of pCREB in oocytes
100
80
60
40
20
0
Control
SQ22536
Forskolin
D
Control
8-Bromo-cAMP
pCREB
DAPI
DIC
Merge
20μm
E
Fluorescence intensity of pCREB in oocytes
80
60
40
20
0
Control
8-Bromo-cAMP
F
Control
H 89 2HCl
pCREB
DAPI
DIC
Merge
20μm
G
Fluorescence intensity of pCREB in oocytes
80
60
40
20
0
Control
H 89 2HCl

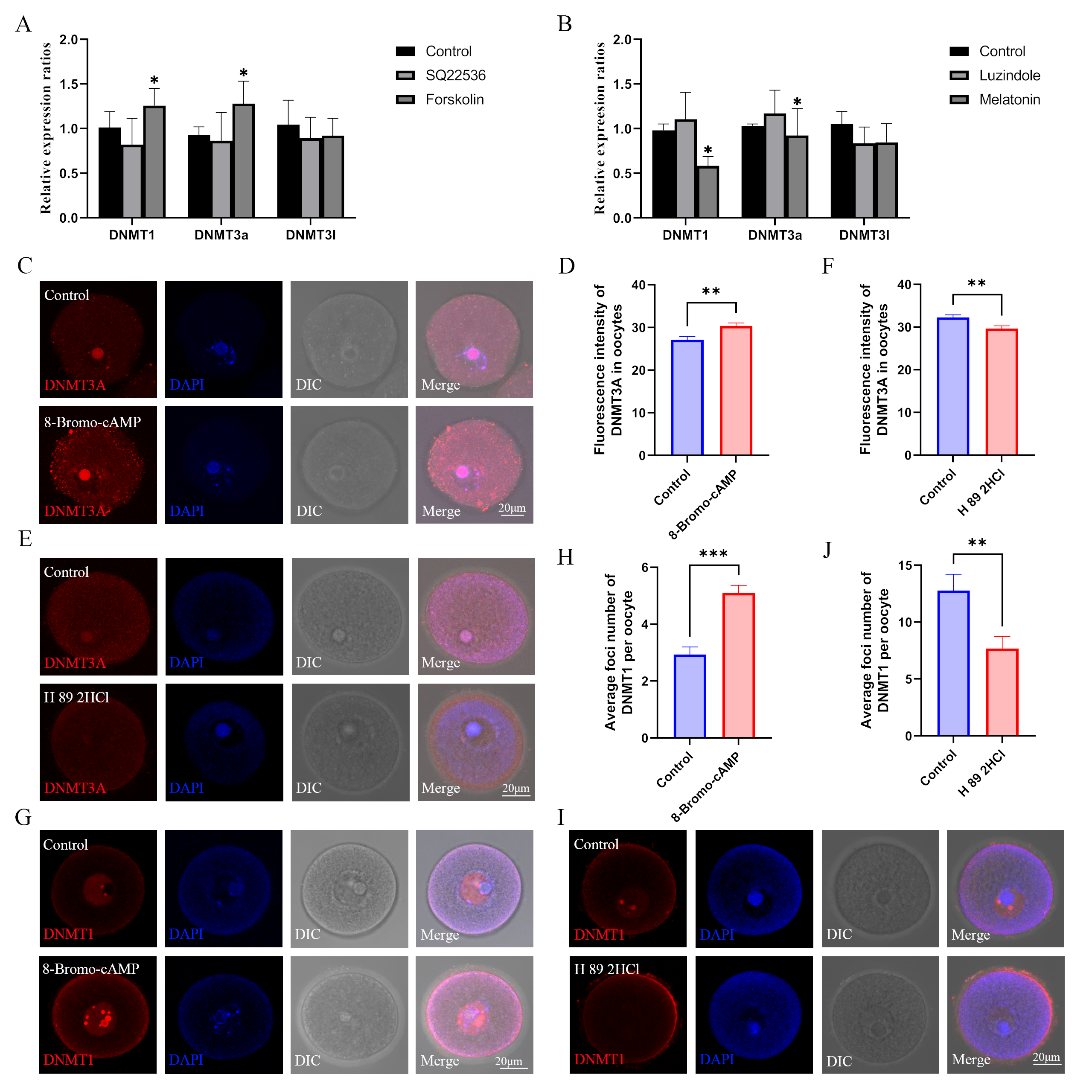
A
Relative expression ratios
2.0
1.5
1.0
0.5
0.0
DNMT1
DNMT3a
DNMT3l
Control
SQ22536
Forskolin
B
Relative expression ratios
Control
Luzindole
Melatonin
C
Control
DNMT3A
DAPI
DIC
Merge
8-Bromo-cAMP
20μm
D
Fluorescence intensity of DNMT3A in oocytes
**
Control
8-Bromo-cAMP
F
H 89 2HCl
E
H
Average foci number of DNMT1 per oocyte
***
J
G
DNMT1
I

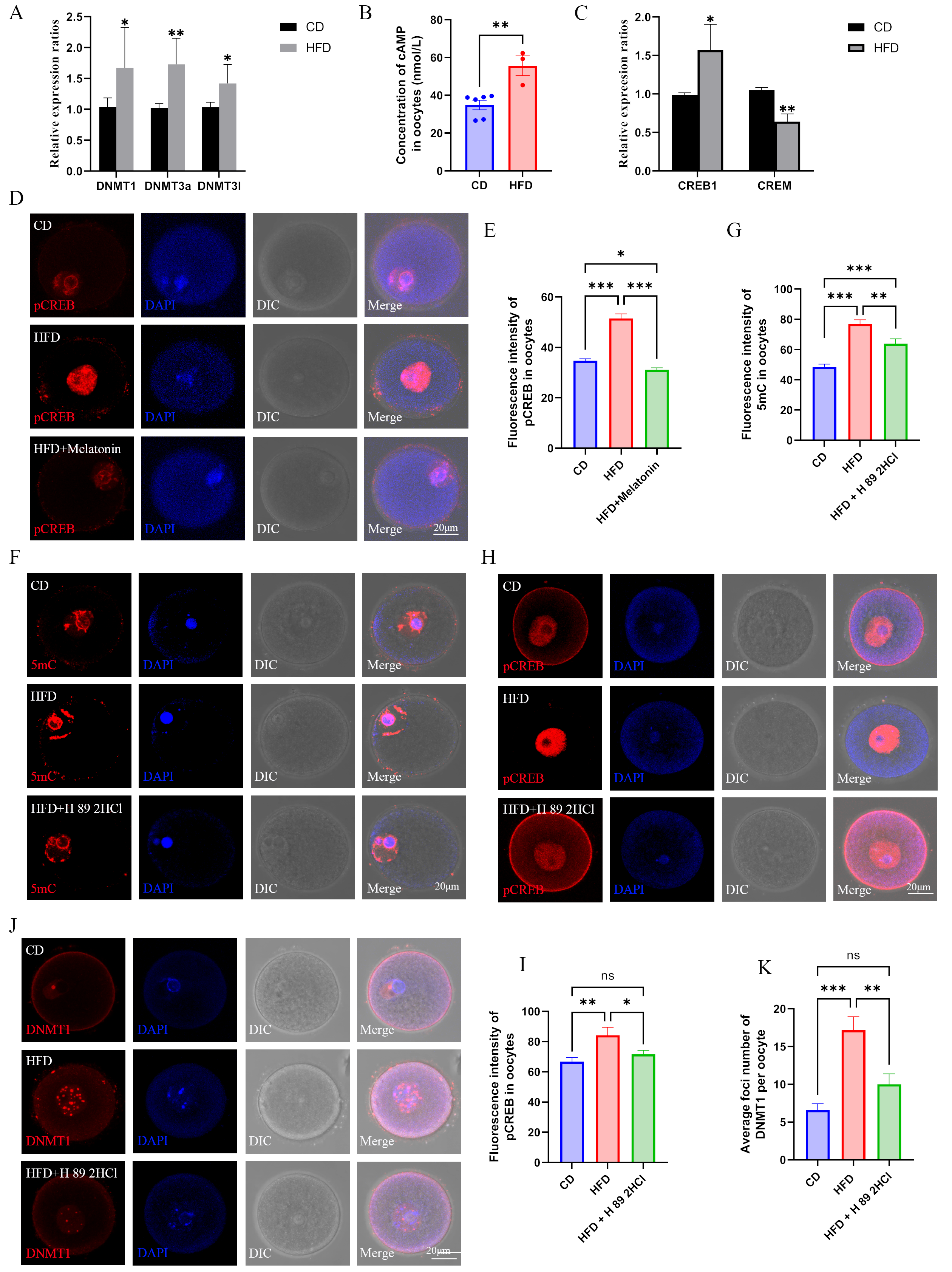
A
Relative expression ratios
DNMT1
DNMT3a
DNMT3l
CD
HFD
B
Concentration of cAMP in oocytes (nmol/L)
CD
HFD
C
Relative expreesion ratios
CREB1
CREM
CD
HFD
D
CD
HFD
HFD+Melatonin
pCREB
DAPI
DIC
Merge
20μm
E
Fluorescence intensity of pCREB in oocytes
CD
HFD
HFD+Melatonin
G
Fluorescence intensity of 5mC in oocytes
CD
HFD
HFD + H 89 2HCl
F
CD
HFD
HFD+H 89 2HCl
5mC
DAPI
DIC
Merge
20μm
H
CD
HFD
HFD+H 89 2HCl
pCREB
DAPI
DIC
Merge
20μm
J
CD
HFD
HFD+H 89 2HCl
DNMT1
DAPI
DIC
Merge
20μm
I
Fluorescence intensity of pCREB in oocytes
ns
CD
HFD
HFD + H 89 2HCl
K
Average foci number of DNMT1 per oocyte
ns
CD
HFD
HFD + H 89 2HCl